We are IntechOpen,
the world's leading publisher of Open Access books
Built by scientists, for scientists

6,900
Open access books available

186,000
International authors and editors

200M
Downloads

154
Countries delivered to

Our authors are among the

TOP 1%
most cited scientists

12.2%
Contributors from top 500 universities

CLARIVATE ANALYTICS
BOOK CITATION INDEX
INDEXED

WEB OF SCIENCE™

Selection of our books indexed in the Book Citation Index
in Web of Science™ Core Collection (BKCI)

Interested in publishing with us?
Contact book.department@intechopen.com

Numbers displayed above are based on latest data collected.
For more information visit www.intechopen.com

Catalytic Natural Gas Utilization on Unconventional Oil Upgrading

Peng He and Hua Song

Additional information is available at the end of the chapter

Abstract

The upgrading of unconventional oil using methane, the principal component of natural gas, is a promising alternative method to the conventional hydrotreating process, which consumes naturally unavailable H_2 at high pressures. Methanotreating is an economically attractive process with abundant and readily available raw materials to accomplish the upgrading of bio-oil and to attain improved oil quality. The application of methane as the H donor avoids the energy consumption and CO_2 rejection during the reforming of methane to produce H_2. More product oil is also obtained through the incorporation of methane into the product oil. Ag/ZSM-5, Zn/ZSM-5 and Ag-Zn/ZSM-5 have been employed to upgrade bio-oil under methane environment to achieve increased oil yield and H/C molar ratio, suppressed total acid number and unsaturation degree of the product oil. Ag-Zn/ZSM-5 is used to catalyze the methanotreating of heavy oil to attain lower viscosity accompanied with good stability and compatibility, which are critical for the pipeline transportation of heavy oil to downstream refineries. Higher gasoline and diesel fractions, increased H/C molar ratio, lower total acid number are witnessed upon the upgrading in the presence of Ag-Zn/ZSM-5 under methane environment. The mechanism studies practiced in the literature using methods including solid-state NMR and FTIR have revealed at least two reaction pathways, i.e., carbenium pathway and alkyl pathway, to accomplish the activation of methane, which is crucial for the involvement of methane in the following upgrading reaction steps. The reaction thermodynamics and reaction intermediates have also been explored by computational approaches by researchers. These observations and achievements will encourage more researchers to develop more catalyst systems and attain improved catalytic performance in the unconventional oil upgrading using natural gas.

Keywords: natural gas, unconventional oil, methane activation, bio-oil, biomass, heavy oil, zeolite, catalytic upgrading, mechanism study, theoretical calculation

1. Introduction

The utilization of unconventional oil is attracting attention as the energy demand is growing rapidly driven by the urbanization all over the world, while the reserve of conventional petroleum is decreasing. The past decade has witnessed a dramatic change brought by unconventional oil to the petroleum industry. For instance, the technology breakthrough in the extraction of shale oil is one of the dominating factors that drive the crude oil price to drop from above 100 USD per barrel in 2014 to below 30 USD per barrel in 2016. Besides shale oil, other unconventional oil resources such as bio-oil and heavy oil could also be the alternative energy source of the conventional petroleum and meet the ever surging demand of human society due to their huge scale of potential reserves.

Bio-oil is receiving increasing attention since it is the only renewable source of hydrocarbon that can be used for liquid fuel [1] and chemical production [2–6] owing to its low cost, ready availability, resource abundance and environment-friendliness [7]. It is often produced from the pyrolysis of biomass, which destructs biomass in the absence of air/oxygen generating liquid bio-oil, syngas and biochar [8]. However, the obtained bio-oil often faces problems such as hydrogen deficit, high oxygen content and the presence of contaminants including sulfur, chlorine and trace metals. The low H/C molar ratio is closely related to the high concentration of unsaturated contents in the bio-oil, resulting in the instability when exposed to light, oxygen or heat above 80°C, rendering stability issues while storage and transportation [9]. The high oxygen content in the bio-oil makes the produced bio-oil of low heating value, impeding its application as substituent for traditional liquid fuel to power the world. In order to deal with these drawbacks, various processes have been explored to remove or chemically modify the undesired components to obtain upgraded bio-oil [10–14], among which hydrodeoxygenation is most widely employed [10–12] to improve the quality of bio-oil in terms of higher energy dense, enhanced stability and suppressed causticity. The process, however, has to consume expensive H_2 at high pressures (typically 70–140 atm and even above 200 atm) [15, 16]. The involvement of naturally unavailable H_2, and the stricter requirements of the reaction units to tolerate high pressure, will eventually escalate the operating cost [15]. The upgrading of bio-oil by catalytic cracking on zeolites at atmosphere pressure without hydrogen has also been explored to produce aromatics [14, 17], which still suffers from the low yield and high coke deposition due to the low H/C molar ratio [18]. Co-feeding with some hydrogen-rich feedstocks such as waste oil, plastics and alcohols can provide hydrogen to the reaction system and improve the quality of bio-oil [19–22]. These co-fed materials, however, are not naturally available on a large scale. Therefore, an economically attractive method with abundant and readily available raw materials to accomplish the upgrading of bio-oil and to attain improved quality is greatly desired.

Another unconventional oil with sufficient potential availability is heavy oil, such as bitumen extracted from Canadian oil sand. There are an estimated 174 billion barrels of bitumen reserves in Canada. In Alberta alone, the bitumen production reached 2.3 million barrels per day in 2014. Compared with conventional petroleum, the deficiency of heavy oil is owing to the low H/C molar ratio, high impurity content, high viscosity, high asphaltene content

and high density [23]. Heavy oil was formed from conventional oil, degraded by bacteria upon the migration towards the surface region. Some light hydrocarbons were consumed during the biology reaction process. As a result, heavy oil is deficient in hydrogen and has high asphaltene content. For instance, the hydrogen to carbon molar ratio is often below 1.5 versus a value close to 2.0 in conventional reservoirs [24]. The heavy oil reservoirs are rich in several countries such as Canada and Venezuela, while the downstream refineries are in other countries including the United States. Therefore, the transportation of heavy oil from the oil fields to refineries is critical for its further upgrading and application in industry. The extracted bitumen from steam-assisted gravity drainage (SAGD) processes in Canada has an average density of 1.0077 g/cm^3, API gravity of 8.9, and a dynamic viscosity of 2×10^5 to 2×10^6 cP at atmospheric conditions [25]. Such a high viscosity makes it challenging to transport heavy oil, especially through pipelines. Dilution of heavy oil is widely practiced to meet pipeline specifications for transport to refineries. Solvents such as naphtha or gas condensates (1:2 ratio of diluent:bitumen, known as dilbit) and synthetic crude oil (SCO) (1:1 ratio of SCO:bitumen, known as synbit) are used to increase the API gravity of the diluted bitumen to 22. Pipeline transport requires a fluid density of <0.940 g/cm^3 and dynamic viscosity of <330 cP (at 7.5–17°C) [25, 26]. Therefore, the complete elimination or significant reduction in diluent usage is highly desired from a financial and operating standpoint as well as from an environmental perspective.

In order to reduce the viscosity, thermal cracking is widely carried out to break down the carbon chains into short ones. Despite the reduced viscosity due to the carbon chain breakage into smaller molecules, the olefin content of the product oil will inevitably be lifted. Olefins contained in the produced oil are oxidatively and thermally unstable and may gradually form polymeric deposit during storage and transportation [27]. Therefore, hydrotreating processes are used to remove the olefin contents and reduce the sulfur and nitrogen content of the oil. But similar to hydrogen oxygenation process on bio-oil, such process is faced by the cost brought by the consumption of naturally unavailable hydrogen as well as the high pressure during the operation.

In industry, more than 50% hydrogen is obtained through the reforming of methane, the principal component of natural gas, such as steam methane reforming of methane. The reforming of methane is a highly endothermic reaction and often requires high operating temperatures (>800°C) and pressures (1.5–3.0 MPa) to attain high equilibrium conversion of CH_4 towards H_2. The involvement of such a naturally unavailable hydrogen source will inevitably result in a significant cost for hydrotreating process. Another drawback of this process is that the carbon from methane has to be ejected as CO_2 to recover H_2, resulting in more greenhouse emission. If CH_4 could be used as the hydrogen source directly in the hydrocracking processes, the operating cost could be lowered, since the cost of methane reforming is saved. In this scenario, rather than ejected as CO_2, the carbon from methane will be incorporated into the product oil to produce more synthetic oil and attain more profit. If the upgrading under CH_4 atmosphere could be achieved at a lowered pressure, the cost of this process would again be reduced since the cost owing to the materials and connections of the reaction units is decreased.

One of the obstacles of the application of methane in oil upgrading is its inert structure. The energy of the C–H bond in methane is the highest among all hydrocarbons. In order to activate the C–H bond of methane for successive upgrading steps, catalysts with high activity and stability should be formulated. Over the past decades, these catalysts that have been intensively studied under variable conditions including oxidation and non-oxidation conditions, shedding light on the oil upgrading using methane. Among them, MIF-type zeolite (ZSM-5)-based catalysts exhibit outstanding methane activation capability under non-oxidation condition, which is more feasible for oil upgrading compared with oxidation condition. These catalysts are prepared by loading active metal species on ZSM-5 framework with variable acidity. At a temperature range of 350–400°C and pressure range of 10–50 bar, these catalysts can catalyze methane to upgrade unconventional oil to achieve the olefin saturation, deoxygenation, desulfurization, denitrogenation and demetallization. These studies open a door for upgrading unconventional oil with natural gas under fairly mild operating conditions instead of expensive hydrogen under rather stringent ones.

2. Production technology overview

2.1. Upgrading technology of bio-oil

Bio-oil is often collected from the pyrolysis of biomass, such as canola straw [28], saw dust [29] and agricultural residues [6], due to the convenient apparatus set up and relatively low capital cost [9]. Bio-oil is produced by heating up the biomass rapidly to a high temperature, typically 450–550°C, for a short period of residence time in the absence of oxygen, followed by the liquid product collection upon condensation [8, 30]. Such a fast pyrolysis process would significantly augment the liquid product yield and suppress the formation of gas product and char [8]. As a sustainable hydrocarbon resource with abundant availability and carbon-neutral nature, bio-oil has drawn attention to be the potential reservoir that provides fuels and chemical feedstocks. The obtained bio-oil is a complex mixture composed of acetic acid, acetaldehyde, water, furfurals and phenolics [31]. The low energy density due to the large amount of oxygenated functional groups and the complex of the product matrix impedes the application of bio-oil as fuels or chemical feedstocks directly. Therefore, lots of efforts have been made to improve the quality of bio-oil in terms of product yield, suitable selectivity, stability, compatibility with conventional fuels, reduced corrosivity and so on.

Nowadays, there are mainly three processes for bio-oil upgrading [30]. In the first one, bio-oil is first produced then upgraded by catalytic cracking, hydrotreating, steam reforming, etc [32]. For instance, the liquefaction oil can undergo the conventional petroleum catalytic hydrotreating method to attain higher yield of hydrocarbons upon deoxygenation [33–35]. Some researchers also put efforts on the catalytic conversion over certain fractions of bio-oil, which is separated from bio-oil by methods rather than distillation of oils. For example, the pyrolysis can be conducted at multiple stages with specific temperatures, resulting in several batches of bio-oil product with different compositions [32]. Upon the fractionation of bio-oil, each fraction can be upgraded more efficiently comparing with the upgrading of bio-oil. Upgrading through reactions such as ketonization of small carboxylic acids [36], aldol

condensation of furfurals followed by hydrogenation [37], alkylation [31] and hydrodeoxygenation [38] of phenolics can be carried out with corresponding high activity catalyst systems, respectively.

The other two processes, called in-bed and in situ pyrolysis, respectively, were divided based on the position of the catalyst within the reactor, while the bio-oil produced by pyrolysis is upgraded in vapor phase at high temperatures [30]. Compared with upgrading after condensation, such vapor phase upgrading is more feasible for industrial application due to the reduced number of operating units. During the in-bed catalytic pyrolysis, biomass and catalyst are mixed together, so the pyrolysis and upgrading are carried out simultaneously. The inorganic components of biomass such as silica, Na, K, Mg and Ca ions might contribute to the upgrading of bio-oil [9]. In the in situ process, the biomass is first cracked to produce pyrolytic vapors, and then the vapors pass through catalyst beds for upgrading. Compared with in-bed process, in this process, the produced bio-char and spent catalyst can be easily separated. Many catalyst systems have been developed to upgrade bio-oil. The co-fed H_2 can enhance the quality of bio-oil by removing the oxygenated function groups via H_2O and CO_2. Many catalyst systems have been developed to achieve desired quality of the bio-oil. Hydrotreating catalysts similar to those used in petroleum industry such as Ni, Co and Mo loaded on silica and alumina supports have been used for the upgrading of bio-oil [9, 39, 40]. Catalysts based on neutral support materials including Ru/C, Pd/C and Pt/C are also used to suppress the coke formation [39, 41]. Other support materials such as ZrO_2, CeO_2, zeolites such as USY [42] and MSU [43] are also used to upgrade bio-oil to increase the product yield and formation of hydrocarbons. Among the catalysts employed, ZSM-5-based catalysts have been widely employed to upgrade bio-oil [12, 30], which might be due to the aromatization capability of ZSM-5 [44].

The in situ pyrolysis apparatus can be modified to execute the bio-oil upgrading using methane, i.e., methanotreating, by replacing H_2 with CH_4, and charging the corresponding catalysts. The flow diagram of a typical reactor system [29] is displayed in **Figure 1**. The biomass, such as saw dust and flex straw, is grounded and sieved into small particles, and then put into the reactor. The biomass particle and the catalyst bed are sandwiched between three layers of quartz wool in the vertically oriented reactor. The feed gas is introduced downstream to react with the vapor product from pyrolysis. The product is then condensed and collected.

It is reported that when Ag/ZSM-5 is charged as the catalyst and sawdust are used as the biomass feedstock, the introduction of CH_4 to the feed gas increases the oil yield from 4.07 to 4.85 wt%. As is displayed in **Table 1**, the quality of the collected oil is also improved. For instance, the H/C molar ratio is increased from 1.29 to 1.76. The contribution due to introduction demonstrates the synergistic effect among methane, biomass pyrolysis and the Ag/ZSM-5 catalyst. When CH_4 is fed without biomass, however, no significant conversion is observed, implying that the presence of biomass is critical to trigger the upgrading process, which relies on the synergetic effect between biomass, methane and the catalyst. It is worth noting that when ZSM-5 is modified by phosphorous and cerium, the oil yield is boosted along with a high H/C molar ratio of 2.26. The improved oil quality might be attributed to the suppressed cracking capability of the catalyst, which reveals a potential direction to optimize the catalyst and achieve a better catalytic performance.
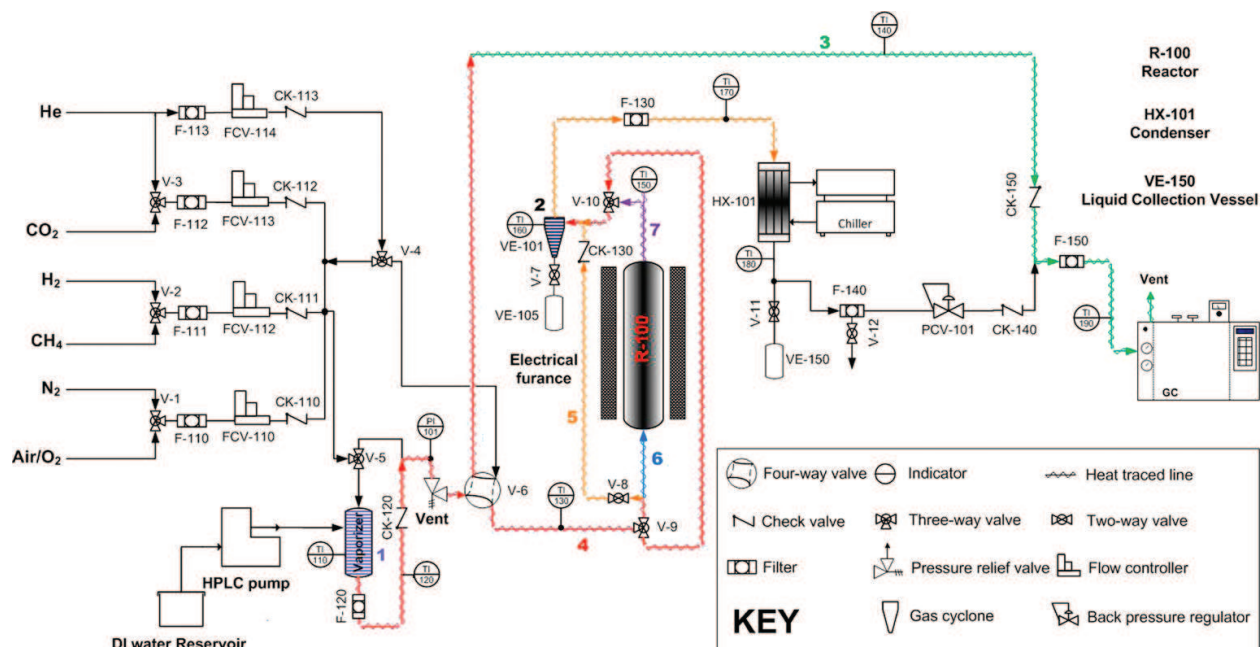
Figure 1. Process flow diagram of a typical multifunctional reactor system. Adapted with permission from Ref. [29]. Copyright 2014 American Chemical Society.

Besides modifying ZSM-5 by silver, the methane catalyzed bio-oil upgrading is also realized by low cost metals [45]. Among Fe, Co, Cu, Mn, Zr, Ni, Ce and Zn, Zn shows the best catalytic performance on bio-oil upgrading when loaded on ZSM-5, in terms of H/C molar ratio, O/C molar ratio and acidity of the product oils. When 5%Zn/ZSM-5 is engaged as the catalyst, the H/C molar ratio of the product oil is increased from 1.92 to 2.20, which is obtained under

Trials	Oil[a]yield (%)	Water formed (mg/g)	Oil quality		
			H/C molar ratio	O content	O/C molar ratio
Inert	5.47	97.0	1.62	5.25	0.226
Inert, Ag/ZSM-5	4.07	135.6	1.29	0.18	0.009
30% H$_2$	4.17	73.4	1.46	3.41	0.145
30% H$_2$, Ag/ZSM-5	3.42	100.2	1.45	0.45	0.024
30% CH$_4$	4.68	119.0	1.38	0.22	0.009
sole 30% CH$_4$, Ag/ZSM-5	4.85	128.3	1.76	0.07	0.003
30% CH$_4$,Ag/P-Ce-ZSM-5	6.89	110.9	2.26	7.35	0.356
30% CH$_4$, Ag/ZSM-5	0	0	—	—	—

Adapted with permission from Ref. [29]. Copyright 2014 American Chemical Society.
[a] Moisture-free liquid collections with boiling point <150°C.

Table 1. Saw dust pyrolysis performance under various environments.

CH_4 environment without catalyst, indicating the incorporation of methane molecules into the product oil. A relatively low total acid number (TAN) of 30.63 mg KOH/g is witnessed along with a low O/C atomic ratio of 0.10, compared with 61.31 mg KOH/g and 0.16 when no catalyst is used under CH_4 environment. The reduced acidity is attributed to the removal of the carboxylic acid groups during the methanotreating. The influence of Zn loading on the catalytic performance is evaluated by varying the loading amount of Zn at 1, 2, 5, 10 and 20 wt%. As is shown in **Figure 2**, the liquid yield increases as the Zn loading is increased to 5%, but start to decrease at 10 and 20%. The H/C molar ratio, on the other hand, reaches the maximum value when the Zn loading is 10%.

By analyzing the products obtained using HZSM-5 and Zn/ZSM-5 with variable metal loading amount, it is concluded that during the reaction ZSM-5 framework promotes the deoxygenation and improves the quality of bio-oil, while the Zn species dispersed on the framework facilitate CH_4 activation and allow it to be incorporated into the carbon chain of the bio-oil, rendering an enhanced quantity of bio-oil.

The upgrading process can also be extended to other fields. For example, the expanding municipal solid waste (MSW) generated during the urbanization all over the work is causing growing environmental risk and management costs. The utilization of MSW in a similar manner as biomass not only disposes of the waste but also supplies the hydrocarbon fuel and chemicals. Therefore, the conversion of MSW into bio-oil upon upgrading under methane environment is drawing attention [28]. When MSW is used as the feedstock, the product oil collected over 1%Ag-5%Zn/ZSM-5 sees an oil yield of 12.73% in the presence of methane. The successful application of the catalytic conversion of MSW into fuels and chemicals under methane might change the landscape of waste management, leading to environmental and economic benefit. It is also worth noting that when MSW is engaged as the feedstock, the presence of 1%Ag-5%Zn/ZSM-5 would enhance the quality of bio-oil compared with 1%Ag/ZSM-5 and 5%Zn/ZSM-5. Transmission electron microscopy (TEM) images (**Figure 3**) coupled with energy dispersive X-ray spectroscopy (EDX) analysis collected over the 1%Ag-5%Zn/ZSM-5 catalyst demonstrate that Ag_2O particles with bigger sizes (about 10–20 nm) are surrounded
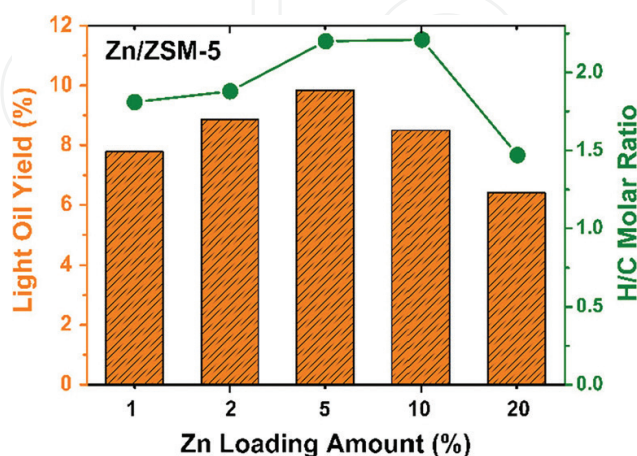

Figure 2. Influence of Zn loading amount on catalytic performance of Zn/ZSM-5. Reprinted from Ref. [45]. Copyright 2015, with permission of Springer.
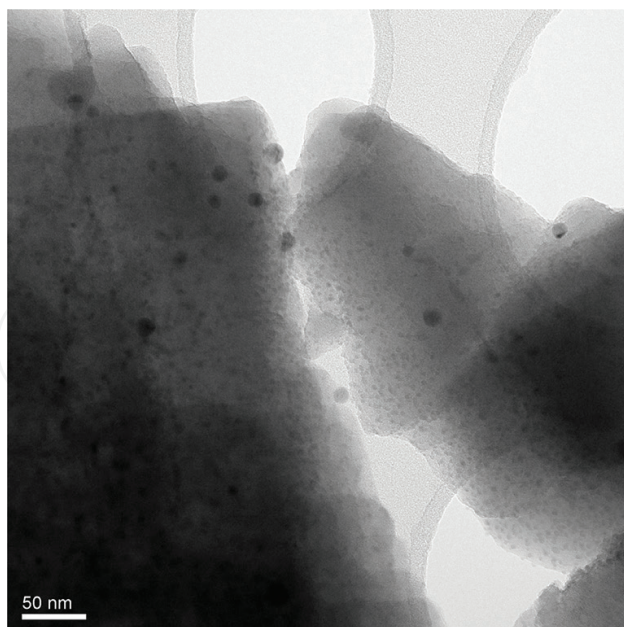
Figure 3. TEM image of 5%Zn–1%Ag/ZSM-5. Reprinted from Ref. [28]. Copyright 2016, with permission of Elsevier.

by the smaller ZnO particles (<10 nm). The synergetic effect due to the two metal species should contribute to the improved catalytic performance.

2.2. Upgrading technology of heavy oil

Hydrotreating is commonly performed to upgrade heavy oil in petroleum industry while hydrodesulfurization, hydrodenitrogenation, hydrodeoxydation and hydrodemetallization take place simultaneously in the presence of catalysts and substantial hydrogen supply. The catalytic hydrotreating capacity in the US is as large as 17.3 million barrels per day in January, 2015, according to the statistics released by the US Energy Information Administration. Olefins, generated during the breaking down of the large molecules in the previous thermal cracking step, are eliminated as hydrogen is added to the unsaturated bonds of olefins [46]. Among the hydrotreating catalysts, catalysts based on Mo_2S promoted with Co or Ni have been intensively investigated for decades due to their good catalytic activity in the hydrotreating processes [47–50]. For instance, the reactivity of the Co-promoted Mo_2S catalyst is believed to be closely related to the Co-Mo-S structure, where the promoter atoms are located on the edge of the MoS_2 clusters [51]. However, MoS_2 promoted hydrotreating process would consume a large amount of hydrogen, which is not naturally available. As is discussed in the previous section, if methane, the principal component of natural gas, can be employed as the H-donor to accomplish methanotreating of heavy oil, the upgrading process can be more profitable and environmental friendly.

Methanotreating of heavy oil has been explored to produce partial upgraded heavy oil, i.e., a product oil with reduced viscosity accompanied along with higher H/C molar ratio, suppressed acidity, improved stability and compatibility, by engaging Ag-Zn/ZSM-5 as the catalyst [52]. As is displayed in **Table 2**, when Ag-Zn/ZSM-5 is charged as the catalyst under an

Trial	Atmosphere	Coke yield (wt.%)	Liquid yield (wt.%)	Viscosity (cP at 25°C)
Bitumen	—	—	—	848,080
–	N_2	0.60	94.5	1718.3
–	CH_4	0.55	96.5	1617.1
HZSM-5	CH_4	0.80	93.8	1374.4
Ag-Zn/ZSM-5	N_2	0.86	92.9	1276.0
Ag-Zn/ZSM-5	CH_4	0.75	97.8	413.7
Ag-Zn/ZSM-5	H_2	0.62	93.1	280.2

Adapted from Ref. [52] with permission from the Royal Society of Chemistry.

Table 2. Performance of bitumen upgrading under various environments at 5.0 MPa and 380 °C for 150 min.

initial CH_4 pressure of 5 MPa, the viscosity of the product oil is remarkably reduced from 848,080 mPa (cP) to 413.7 cP, approaching the pipeline transportation requirements [53]. Despite a lower viscosity is witnessed when H_2 is employed in the reaction, the liquid product yield is higher when CH_4 is used, which is assigned to the incorporation of methane molecules into the product. The stability and compatibility of the collected product oil are evaluated through spot test. The obtained spot test images (**Figure 4**) show that the oil product collected under CH_4 environment with the Ag-Zn/ZSM-5 charged (**Figure 4e**) exhibits the best stability and compatibility which approach those of the product from the H_2 run (**Figure 4f**) making it more suitable for pipeline transportation.

Besides viscosity and stability, gasoline and diesel fractions of the oil samples also get significantly improved upon the methanotreating. Because the heavy oil will eventually be converted to gasoline and diesel in downstream refineries, an increased gasoline and diesel fraction in the
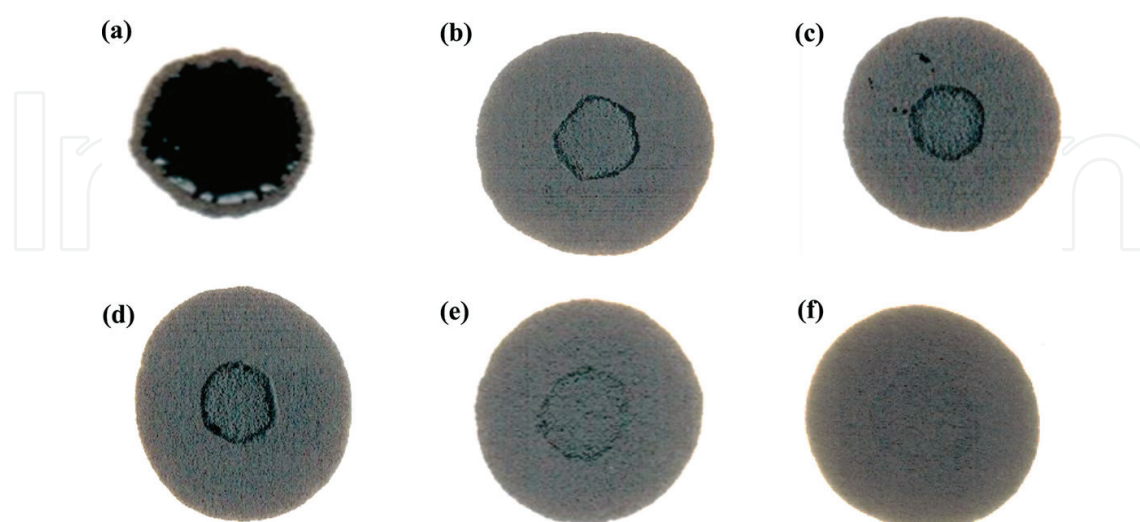

Figure 4. Stability test of (a) heavy oil feedstock and oil products collected under (b) N_2, (c) CH_4, (d) CH_4 with ZSM-5, (e) CH_4 with the Ag-Zn/ZSM-5 catalyst, and (f) H_2 with the Ag-Zn/ZSM-5 catalyst. Adapted from Ref. [52] with permission from the Royal Society of Chemistry.

product oil would lessen the burden of downstream refineries and make the partial upgrading more profitable. The gasoline and diesel fractions of the bitumen feedstock and the product oils gained under variable conditions are presented in **Table 3**. In the bitumen feedstock, there is litter gasoline and a small fraction of diesel (11.96%). After upgrading under various conditions, such as thermocracking under N_2 or CH_4, and catalytic upgrading under N_2 or CH_4, the fraction of gasoline and diesel is increased. However, among the oils in comparison, the highest total gasoline and diesel fraction of 36.77% and the highest gasoline fraction of 13.38% are achieved upon the upgrading in the presence of methane and the catalyst Ag-Zn/ZSM-5, demonstrating the carbon chain breakage and rearrangement capability of the catalyst under CH_4.

Other properties of the oil including density, total acid number (TAN), water content, averaged molecular weight and asphaltene content are critical for the pipeline transportation. Therefore, they are also important criteria for the industry application of the partial upgrading. These parameters of the bitumen feedstock and product oils are summarized in **Table 4**. After upgrading in the presence of methane and Ag-Zn/ZSM-5, the density is lowered from 1.0275 to 0.9668 g/cm³⁰, corresponding to an API of 14.7. The reduced density is consistent with the increased gasoline and diesel fraction. These improved parameters can be attributed to the cracking capacity of the catalyst under CH_4, which is further evidenced by the averaged molecular weight of the product oil. The lowest molecular weight (330 g mol⁻¹) belongs to the oil product obtained under CH_4 with the Ag-Zn/ZSM-5 present. Among the product oil samples in comparison, the increased water content is accompanied by the reduced TAN. When upgrading occurs under the environment of methane with the facilitation of the catalyst, TAN is dramatically scaled down from 2.59 to 0.03 mg KOH/g, which results from the hydrodeoxygenation reactions that consume carboxylic and hydroxyl groups during methanotreating. The content of asphaltenes, the major contributor to the high viscosity of bitumen and the most difficult component in bitumen to be upgraded, of the various oil products is also compiled in **Table 4**. The methanotreatment witnesses a profound effect on the asphaltene content from 22.04 to 12.32%, which is a 44.1% reduction with respect to that of bitumen feedstock. This phenomenon is one important factor that contributes to the viscosity reduction in the product oil.

Trial	Atmosphere	Gasoline (wt.%)	Diesel (wt.%)	Total gasoline and diesel (wt.%)
Bitumen	–	0.19	11.96	12.15
–	N_2	6.88	20.81	27.69
–	CH_4	6.95	23.74	30.69
HZSM-5	CH_4	6.47	25.26	31.73
Ag-Zn/ZSM-5	N_2	6.28	26.57	32.85
Ag-Zn/ZSM-5	CH_4	13.38	23.39	36.77

Adapted from Ref. [52] with permission from the Royal Society of Chemistry.

Table 3. Gasoline and diesel fractions of the oil samples collected before and after bitumen upgrading under various environments at 5.0 MPa and 380°C for 150 min.

Oil sample	Liquid product properties				
	Density (g/cm³)	TAN (mg KOH/g)	Water content (wt.%)	Molecular weight (g/mol)	Asphaltene content (wt.%)
Bitumen	1.0275	2.59	0.159	700	22.04
N$_2$	0.9957	0.51	0.147	527	16.81
CH$_4$	0.9871	0.24	0.162	541	16.12
CH$_4$+ZSM-5	0.9762	0.26	0.171	524	14.84
N$_2$+ Ag-Zn/ZSM5	0.9755	0.39	0.158	458	14.43
CH$_4$+ Ag-Zn/ZSM5	0.9668	0.03	0.185	330	12.32

Adapted from Ref. [52] with permission from the Royal Society of Chemistry.

Table 4. Properties of the oil samples collected before and after bitumen upgrading under various environments at 5.0 MPa and 380°C for 150 min.

The element composition of the product oils are listed in **Table 5** for comparison. When Ag-Zn/ZSM-5 is present with CH$_4$, the highest H/C molar ratio of the product oil is obtained at 1.65, compared with 1.52 in bitumen feedstock. The increased H/C obtained over this reaction condition verifies the participation of methane in the reaction and implies its incorporation into the product oils. Besides, the H/C molar ratio is closely related to the saturation degree of the product oil, which plays an important role in its stability. Therefore, a high H/C molar ratio is favorable for the storage and transportation of the product oil. The increased H/C molar ratio is also accompanied with decreased nitrogen and sulfur content, indicating a spontaneous denitrogenation and desulfurization, which will ease the work load of oil upgrading in downstream refineries.

Oil sample	Carbon (wt.%)	Hydrogen (wt.%)	H/C molar ratio	Nitrogen (wt.%)	Sulfur (wt.%)
Bitumen	81.09	10.29	1.52	1.85	6.48
N$_2$	81.96	10.44	1.53	1.74	5.58
CH$_4$	81.88	10.28	1.51	1.78	5.81
CH$_4$+ZSM-5	81.93	10.19	1.49	1.84	5.74
N$_2$+Ag-Zn/ZSM5	81.66	10.48	1.54	1.73	5.89
CH$_4$+Ag-Zn/ZSM5	81.34	11.18	1.65	1.72	5.58

Adapted from Ref. [52] with permission from the Royal Society of Chemistry.

Table 5. Elemental analysis of oil samples collected before and after bitumen upgrading under various environments at 5.0 MPa and 380°C for 150 min.

3. Catalyst structure and optimization

The key to upgrade unconventional oils lies on the catalyst that can effectively activate methane. The catalyst should possess the capacity to rearrange carbon chains. Several catalysts have been successfully employed to upgrade bio-oil and heavy oil using methane, such as

Ag/ZSM-5, Zn/ZSM-5 and Ag-Zn/ZSM-5. Their catalytic performance, which has been discussed in the previous section, is closely associated with their unique structures. Therefore, the structure characterization is fundamental to get a better understanding of the reaction mechanisms, leading to a rational design of the catalyst formula to achieve improved catalytic performance.

3.1. 1%Ag/ZSM-5

1%Ag/ZSM-5 has been used to upgrade the bio-oil generated by the fast pyrolysis of biomass in vapor phase [29]. It is prepared by the incipient wetness impregnation of HZSM-5 with $AgNO_3$ solution, followed by calcination at high temperatures for 3 h [29]. One structure parameter that has profound influence on the catalytic performance is the dispersion of the active metal, which can be promoted by optimizing the precursor solution concentration (**Figure 5a**) and calcination temperature (**Figure 5b**). When the precursor concentration is 0.1 mol/L and the calcination temperature is 600°C, the magnitude of Ag dispersion is maximized. The Ag particles are widely dispersed throughout the catalyst surface with an averaged diameter of 13 nm (**Figure 6a**). Another approach to improve the catalytic performance of the catalyst is by introducing promoters to the catalyst. When the support is modified by phosphorous and cerium, the morphology of the catalyst is changed dramatically (**Figure 6b**). The irregularly shaped zeolite support is surrounded by many needle-shaped rods agglomerated into small clusters, which are mainly composed of cerium oxide with small decoration of phosphorus oxide, accompanied by the presence of silver species. As a result, significantly enhanced H/C ratio as well as oil yield is witnessed upon the structure modification (**Table 1**).
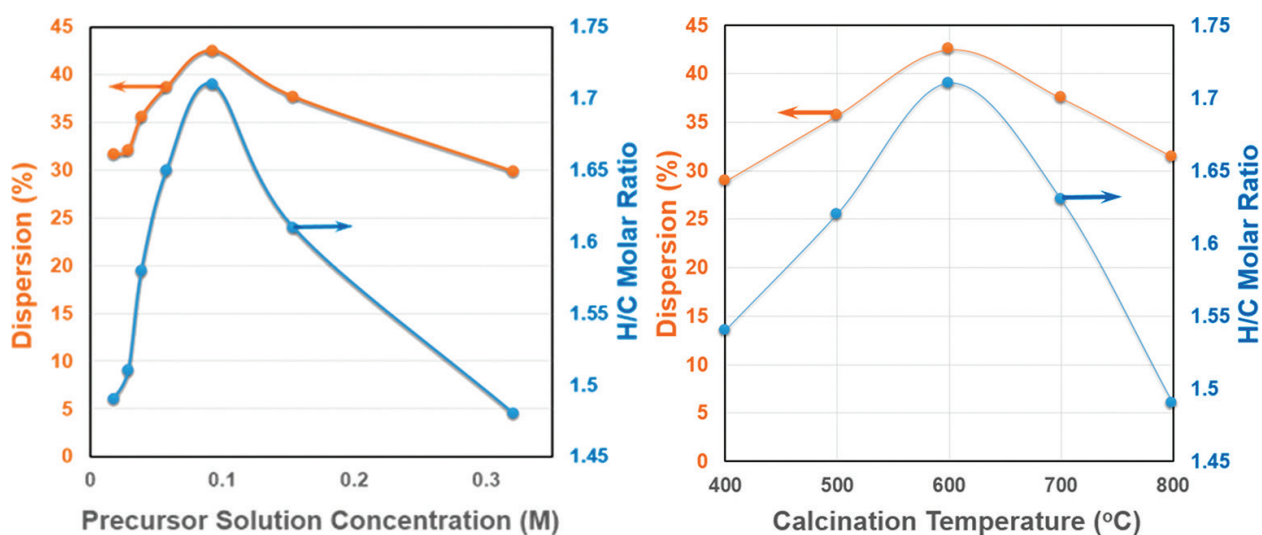

Figure 5. The Ag dispersion and H/C atomic ratio as a function of (a) $AgNO_3$ concentration (calcination temperature is 600°C) and (b) calcination temperature ($AgNO_3$ precursor concentration is 0.1 M) used for Ag/ZSM-5 synthesis. Adapted with permission from Ref. [29]. Copyright 2014 American Chemical Society.
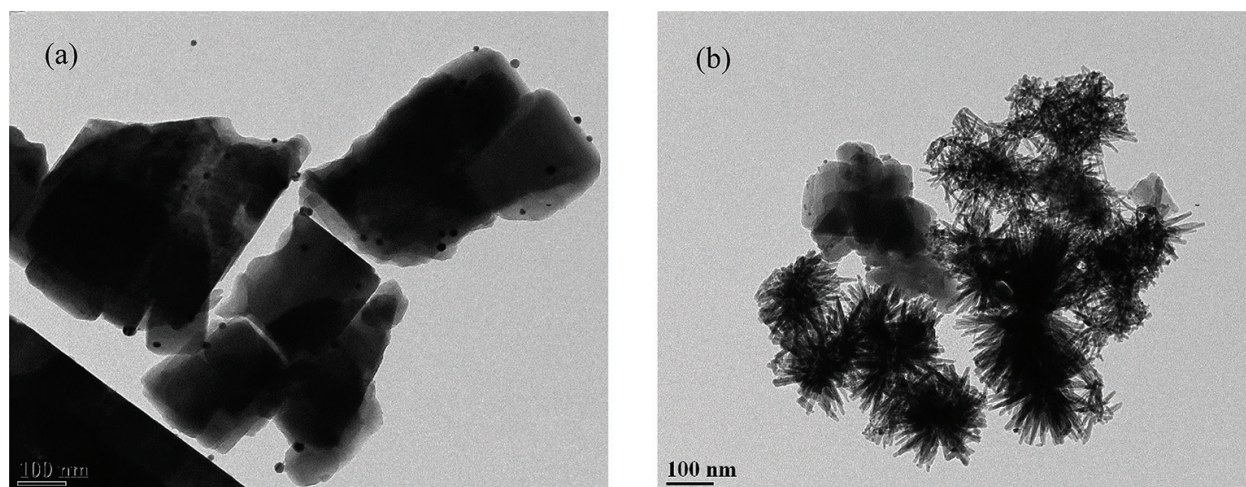
Figure 6. TEM images of the fresh catalysts of Ag/ZSM-5 (a) and Ag/P-Ce-ZSM-5 (b). Adapted with permission from Ref. [29]. Copyright 2014 American Chemical Society.

3.2. 5%Zn/ZSM-5

Besides 1%Ag/ZSM-5, 5%Zn/ZSM-5 is also used to upgrade the bio-oil [45]. As is discussed in the previous section, the loading amount of Zn is selected to be 5wt% based on the oil yield and H/C molar ratio of the product oil (**Figure 2**). The XRD patterns of HZSM-5 and the catalysts are displayed in **Figure 7**. When Zn loading is 1, 2 and 5%, no additional peak is observed, indicating the Zn species is well-dispersed. When Zn loading is increased to 10%, the diffraction peaks due to ZnO crystalline start to appear and become noticeable when the loading is increased to 20%. The averaged particle sizes of ZnO are calculated to be 15.9 and 38.4 nm, respectively. The TEM image of 5%Zn/ZSM-5 (**Figure 8**) shows that the ZnO particle size is below 10 nm. The smaller particle size and better dispersion should benefit and contribute to the outstanding performance of 5%Zn/ZSM-5.

Figure 7. XRD patterns of H-ZSM-5 and Zn/ZSM-5 catalysts. Adapted with permission from Ref. [29]. Copyright 2014 American Chemical Society.
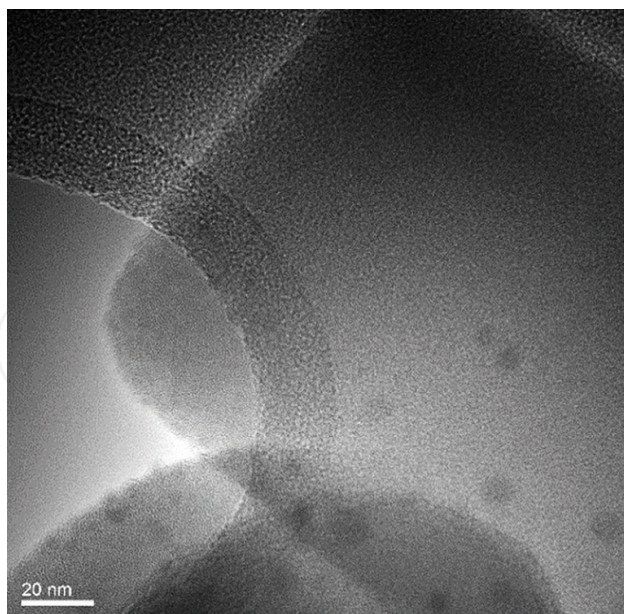
Figure 8. TEM image of 5%Zn/ZSM-5 catalyst. Adapted with permission from Ref. [29]. Copyright 2014 American Chemical Society.

3.3. Ag-Zn/ZSM-5

By combining Ag and Zn to modify HZSM-5, Ag-Zn/ZSM-5 has been employed to upgrade bio-oil and heavy oil [28, 52]. The XRD pattern of 1%Ag-5%Zn/ZSM-5 is present in **Figure 9**. At this loading amount, no additional peak besides those belonging to the HZSM-5 support is observed, indicating that the metal particles are well-dispersed. The averaged particle size of Ag and Zn oxide species are determined from the TEM coupled with EDX images (**Figure 3**). The element composition of the particles can be determined by the EDX spectra (**Figure 10**). It is demonstrated that Ag_2O particles with bigger sizes (about 10–20 nm) are surrounded by the ZnO particles with smaller sizes (<10 nm).

Figure 9. XRD patterns of the catalyst samples. Reprinted from Ref. [28]. Copyright 2016, with permission of Elsevier.
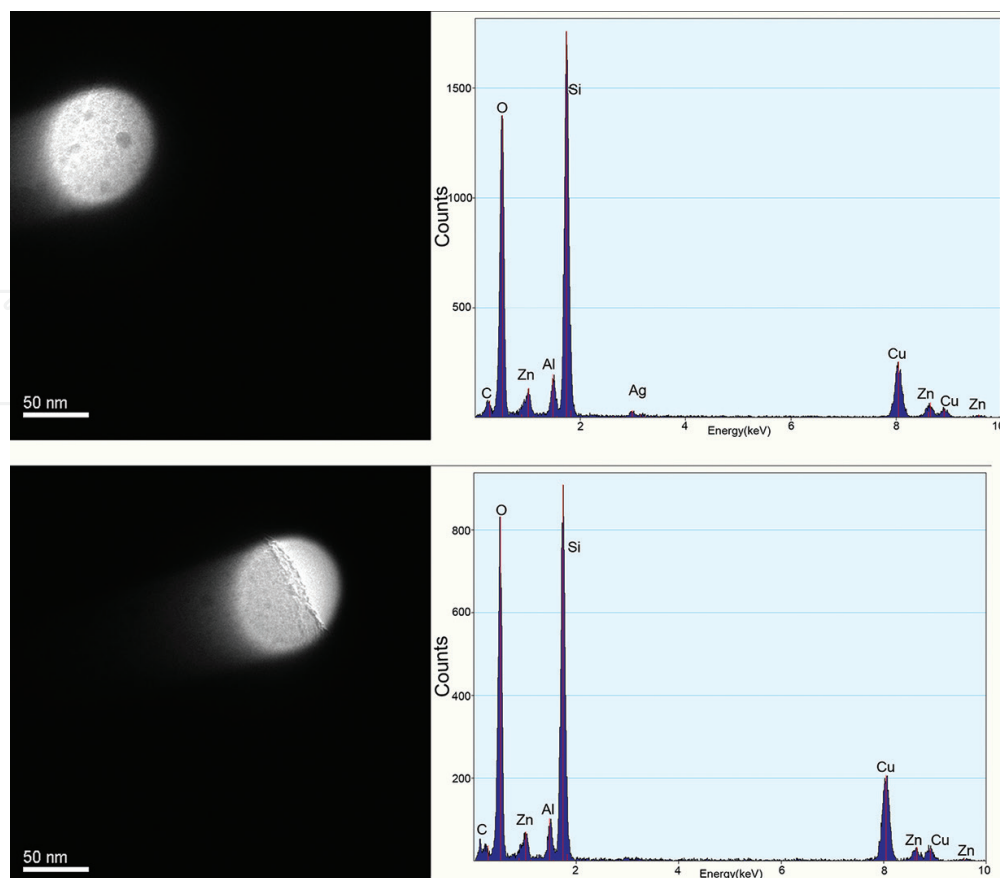
Figure 10. TEM–EDX results of different area for 5%Zn–1%Ag/ZSM-5. Reprinted from Ref. [28]. Copyright 2016, with permission of Elsevier.
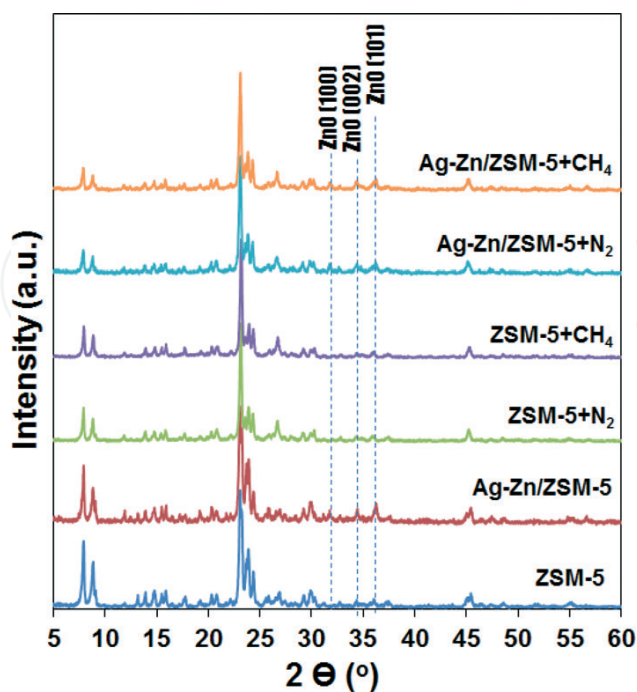

Figure 11. XRD patterns of ZSM-5 and Ag-Zn/ZSM-5 before and after n-butylbenzene upgrading at 3.0 MPa and 380°C for 150 min. Adapted from Ref. [52] with permission from the Royal Society of Chemistry.

XRD patterns and TEM images of the 1%Ag-10%Zn/ZSM-5, which is used to catalyze the methanotreating of heavy oil, are also acquired to investigate the behavior of the catalyst during the upgrading. **Figure 11** shows the XRD spectra of HZSM-5 and Ag-Zn/ZSM-5 acquired before and after the reaction with n-butylbenzene, a model compound to represent heavy oil, under N_2 and CH_4. It is noticed that diffraction peaks of Ag species are not discernible owing to its low loading and high dispersion. Also, the patterns of HZSM-5 remain unchanged upon metal loading and reaction, indicating that the catalyst structure remains intact after the introduction of metal species and the reaction. The diffraction peaks of ZnO, on the other hand, become smaller and wider after reaction, implying the reduction in Zn species and improved dispersion during the reaction.
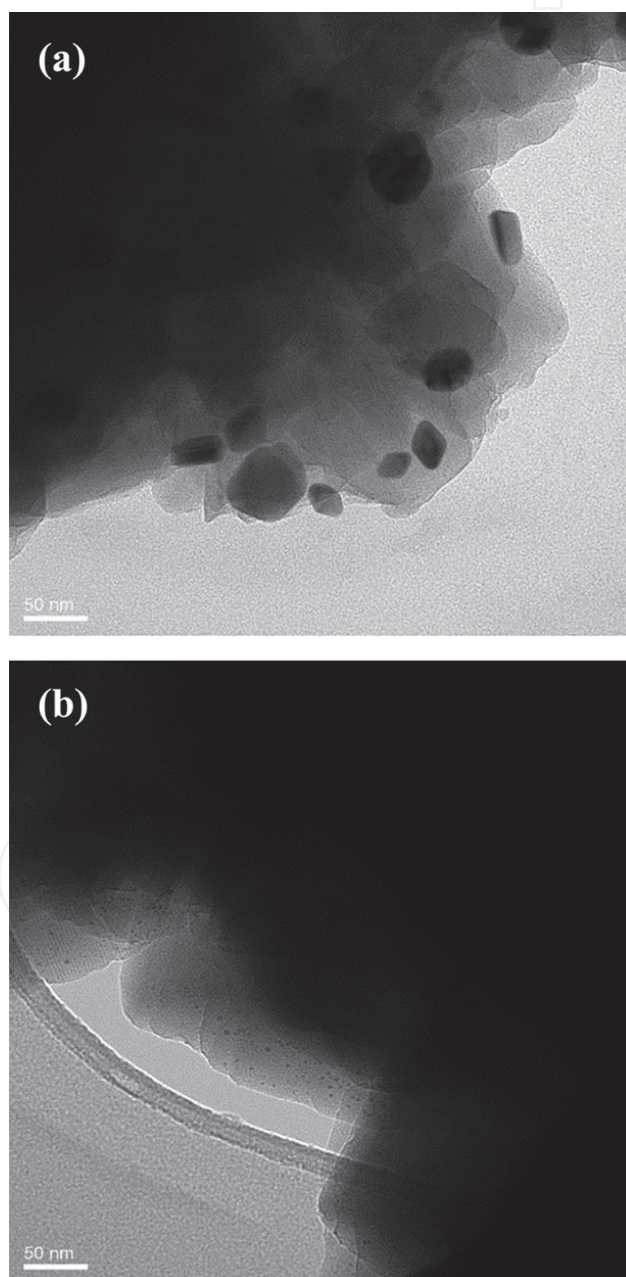

Figure 12. TEM images of spent Ag-Zn/ZSM-5 collected after catalytic n-butylbenzene cracking under the environment of (a) N_2 and (b) CH_4. Adapted from Ref. [52] with permission from the Royal Society of Chemistry.

The improved dispersion of ZnO is evidenced on the TEM image (**Figure 12**) acquired over Ag-Zn/SM-5 after the reaction under CH_4, while significant agglomeration of ZnO is witnessed under N_2. The improved ZnO dispersion assisted by CH_4 might be the reason for the catalytic upgrading performance under CH_4 environment.

4. Reaction mechanism study

The mechanism study of the reaction pathway is crucial for the rational design of the catalyst formula to achieve improved catalytic performance. Several methods have been carried out to probe the reaction pathway and approach the detailed information during the reaction.

Diffuse reflectance infrared Fourier transform (DRIFT) spectroscopy is employed to study the heavy oil upgrading mechanism on the surface of 1%Ag-10%Zn/ZSM-5 [52]. The FTIR spectra of the surface species on the catalysts at a series of stages of the reaction are collected. By comparing the spectra collected with and without methane, the interaction between the catalyst and methane are revealed. Considering the complex nature of the heavy oil matrix, styrene is chosen as the model compound to represent the reactive compounds in heavy oil during the methanotreating. The DRIFT spectra acquired from the styrene temperature-programmed desorption (TPD) experiment under N_2 (blue line) and CH_4 (red line) environment are displayed in **Figure 13**. The peaks assigned to various bonds are labelled by dots with different colors. The blue dot represents C–H stretching at 3015 cm^{-1} due to the presence of methane in the gas phase. The brown dot represents the peaks due to C–O bending derived from styrene adsorption on the surface of Ag-Zn/ZSM-5, which decay much faster when CH_4 is present. This phenomenon implies that when CH_4 is present, the adsorbed styrene surface species
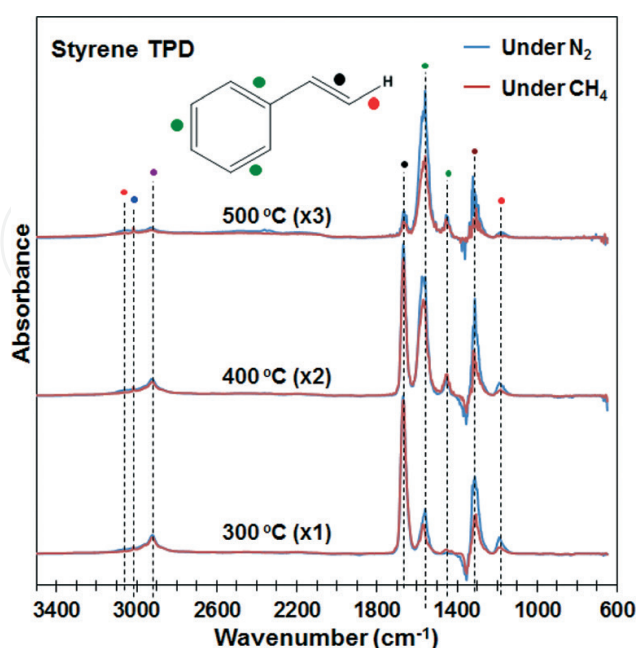

Figure 13. DRIFT spectra collected at different temperatures during styrene saturation under various gas environments over Ag–Zn/ZSM-5. Adapted from Ref. [52] with permission from the Royal Society of Chemistry.

would react with CH_4 and leave the catalyst surface. Similarly, the peaks due to the vinyl groups and aromatics also get smaller under CH_4 compared with the N_2 counterpart. And the reduced peak intensity is more significant at higher temperatures, i.e., 400 and 500°C. Such observations evidence the interaction between CH_4 and the styrene surface species on Ag-Zn/ZSM-5 and show that the reaction is more active at higher temperatures.

The reaction taking placing on the catalyst is also investigated by X-ray photoelectron spectroscopy (XPS). The spectra of the fresh and spent Ag-Zn/ZSM-5 obtained after the upgrading of n-butylbenzene under CH_4 and N_2 environment are presented in **Figure 14**. On **Figure 14a**, the peaks due to Ag 3d shift towards higher binding energy, indicating the reduction in the Ag species, which is one part of the upgrading process. The decreased amount of Ag and Zn species upon the reaction is also witnessed in **Figure 14a** and **b**. It could be due to the diffusion of the metal species into the inner pores. Nevertheless, higher concentrations of Ag and Zn remain on the surface of the catalyst when CH_4 is present, which might be correlate to the better performance under CH_4 environment. The reduction in O concentration is also seen after the loading of metal species (**Figure 14c**), which might be due to the occupation of oxygen sites by the metals. After the reaction, the remaining oxygen concentration is higher with the presence of CH_4, which can be correlated to its better catalytic performance.

The mechanism is probed by the GC-MS analysis of the product oil obtained by the upgrading of n-butylbenzene over various conditions. The results are shown in **Table 6**.
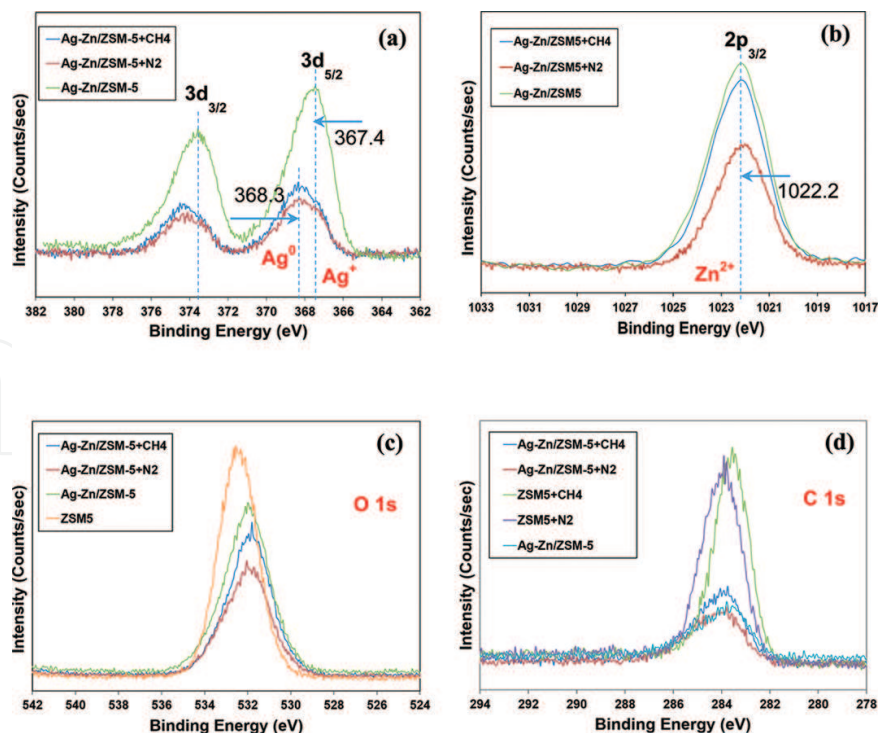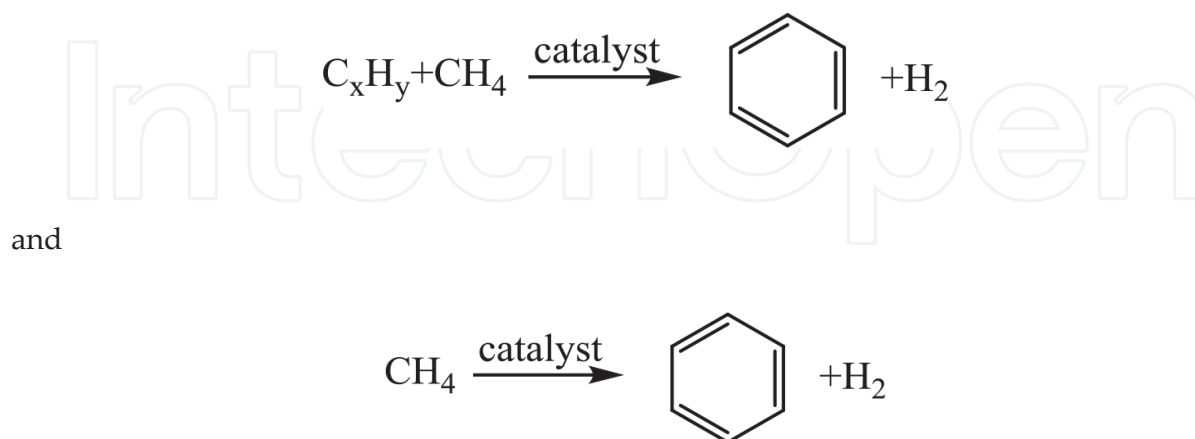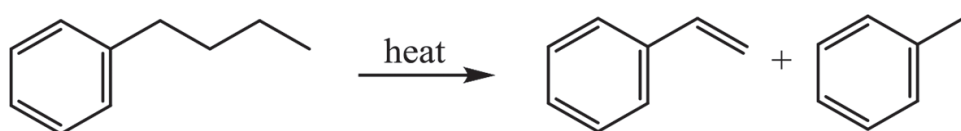

Figure 14. XPS spectra of HZSM-5 and Ag-Zn/ZSM-5 before and after n-butylbenzene upgrading at 3.0 MPa and 380°C for 150 min under different environments at (a) Ag 3d, (b) Zn 2p, (c) O 1s, and (d) C 1s regions. Reproduced from Ref. [52] with permission from the Royal Society of Chemistry.
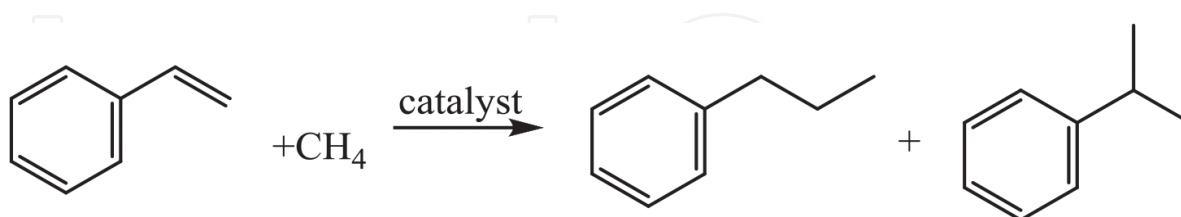
It is clear that the portion of benzene in the product is significantly increased when Ag-Zn/ZSM-5 is charged in the presence of CH_4. It can be attributed to the aromatization of methane under the non-oxidative environment, which has been studied intensively [54–59]. There are at least two possible pathways, i.e.,
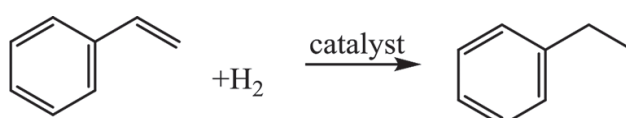
$$C_xH_y + CH_4 \xrightarrow{\text{catalyst}} \text{⬡} + H_2$$

and

$$CH_4 \xrightarrow{\text{catalyst}} \text{⬡} + H_2$$

It is observed that styrene is the primary product of the thermocracking

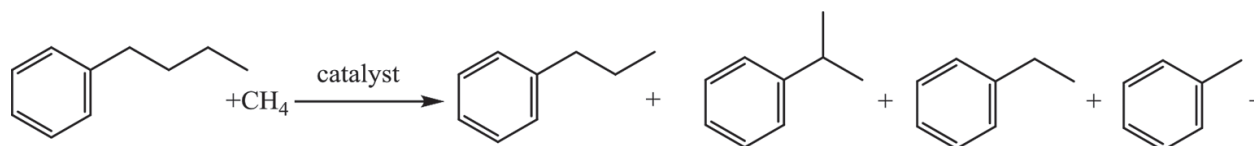$$\text{⬡—CH}_2\text{CH}_2\text{CH}_3 \xrightarrow{\text{heat}} \text{⬡—CH=CH}_2 + \text{⬡—CH}_3$$

It is also interesting to note that the ratio between isopropylbenzen and styrene, and that between n-propylbenzene and styrene, are 2.5 and 8.4 when the catalyst is charged under N_2 environment. The ratios are increased to 11.3 and 45.9 when CH_4 is present. The higher ratios are due to the addition of CH_4 into the vinyl group of styrene:

$$\text{⬡—CH=CH}_2 + CH_4 \xrightarrow{\text{catalyst}} \text{⬡—CH}_2\text{CH}_2\text{CH}_3 + \text{⬡—CH(CH}_3)_2$$

Another interesting observation is that ethylbenzene, which is absent under N_2 environment, appears when CH_4 is present. It can be because that the H_2 formed during the CH_4 dissociation is added to styrene:

$$\text{⬡—CH=CH}_2 + H_2 \xrightarrow{\text{catalyst}} \text{⬡—CH}_2\text{CH}_3$$

Based on these observations and interpretations, the overall reaction can be summarized to be

Compound	Liquid product distribution/conversion (wt%)					
	N_2	CH_4	ZSM-5, N_2	ZSM-5,CH_4	Ag-Zn/ZSM-5, N_2	Ag-Zn/ZSM-5, CH_4
Benzene	0.58	0.61	29.50	28.98	37.86	45.88
Methylbenzene	30.34	31.33	1.70	1.28	2.33	2.28
Ethylbenzene	1.36	1.32	2.32	4.10	0	0.82
Styrene	19.59	19.78	0	0	0.71	0.12
Isopropylbenzene	0	0	8.94	9.79	1.74	1.35
N-propylbenzene	0	0	0	0	5.97	5.51
Pentylbenzene	3.05	2.95	1.76	4.00	3.39	2.16
Heptylbenzene	0	0	9.00	7.37	15.56	13.22
Octylbenzene	0	0	3.66	1.74	20.74	16.26
Nonylbenzene	0	0	0	2.75	3.81	2.59
Butylbenzene[a]	0.89	0.81	88.71	86.43	21.94	25.04
Methane[a]	–	0	–	0	–	10.84

Adapted from Ref. [52] with permission from the Royal Society of Chemistry.

[a] Conversion.

Table 6. Composition of liquid products and conversions of n-butylbenzene and methane at 5.0 MPa and 380°C for 150 min.
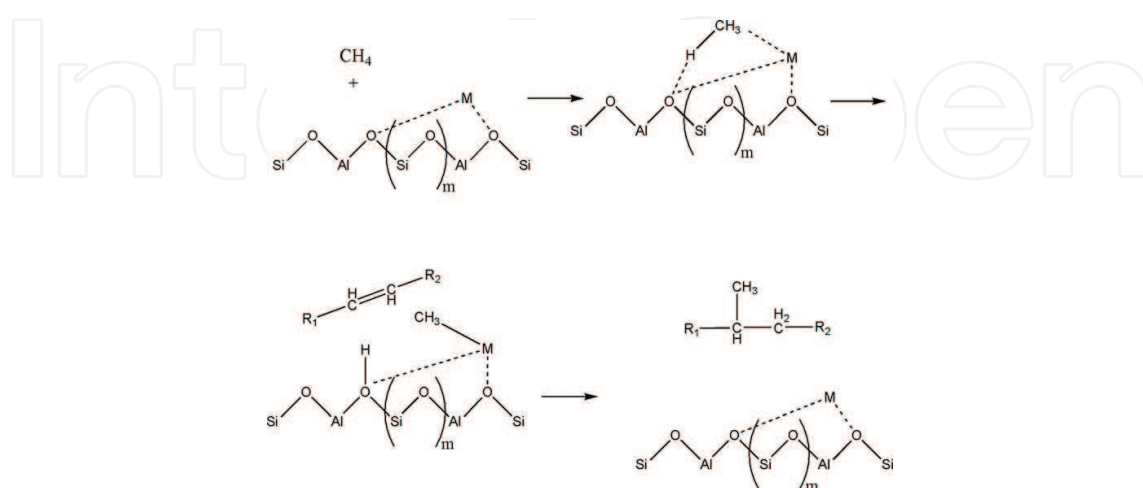

Figure 15. The hypothetical reaction mechanism of methane activation and addition to the broken pieces formed during hydrocarbon cracking over Ag–Zn/ZSM-5 (M=Zn^{2+} or Ag^+). Reproduced from Ref. [52] with permission from the Royal Society of Chemistry.
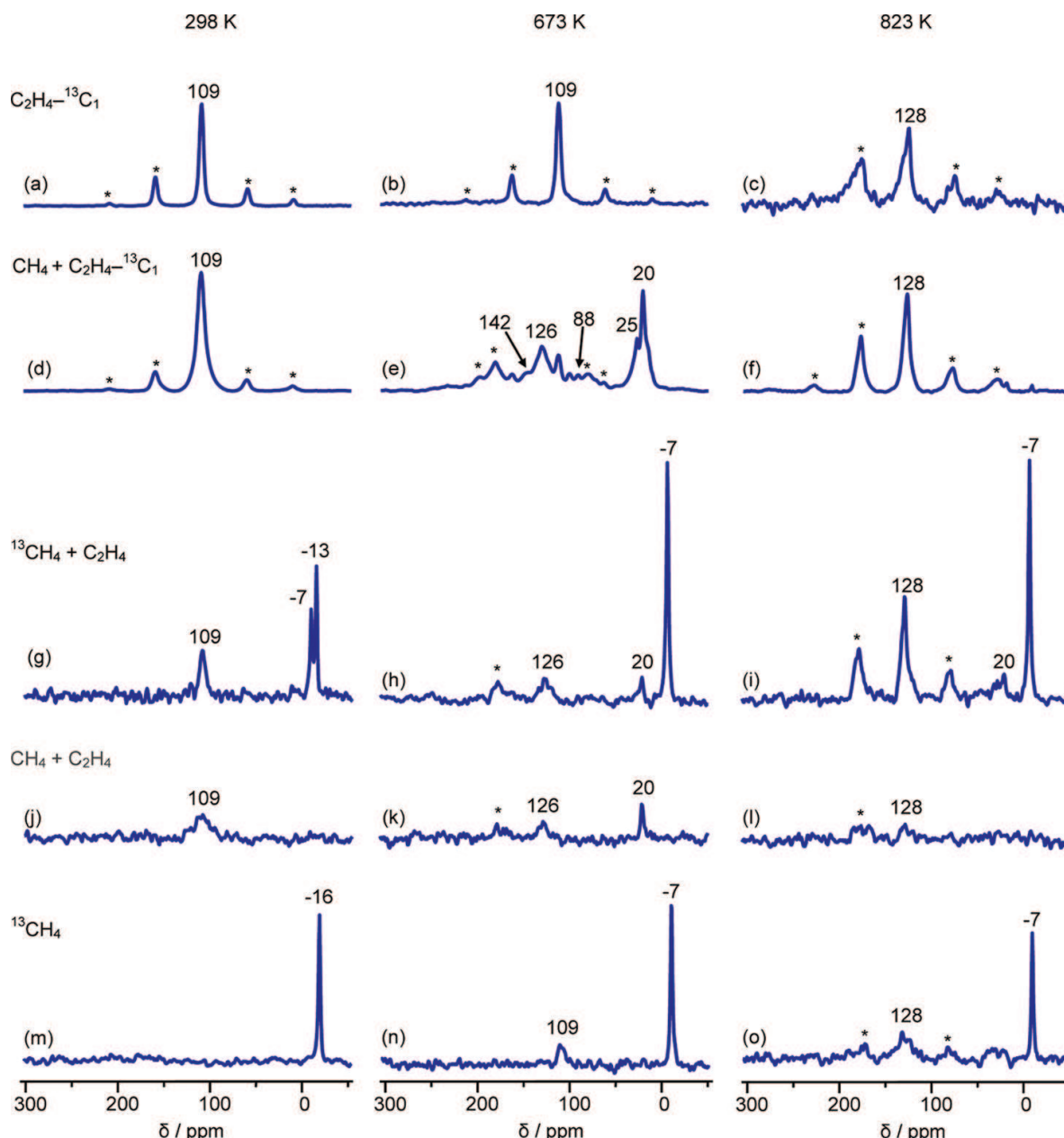
Figure 16. ^{13}C CP/MAS NMR spectra of methane and ethene adsorbed on Ag/H-ZSM-5 at room temperature and heated for 15 min at 673–823 K. Ethene-$^{13}C_1$ was heated at 298 (a), 673 (b), and 823 K (c). Methane and ethene-$^{13}C_1$ were heated at 298 (d), 673 (e), and 823 K (f). Methane-^{13}C and ethene were heated at 298 (g), 673 (h), and 823 K (i). Methane and ethene were heated at 298 (j), 673 (k), and 823 K (l). Methane was heated at 298 (m), 673 (n), and 823 K (o). Spectra g–o were acquired under identical conditions, with 3000 scans and a repetition time of 2 s. Asterisks denote the spinning side bands. Adapted with permission from Ref. [64]. Copyright 2013 American Chemical Society.

The reaction mechanism is proposed as **Figure 15**.

The reaction mechanism of oil upgrading using methane is also approached from the perspective of methane activation, which is the key step involved. By simplifying the feedstock system, the revolution of methane can be tracked more accurately. Among the methods, solid-state NMR (SSNMR) has been widely used to probe the reaction intermediates [60–63]. For instance, Gabrienko et al. [64] has used ^{13}C-enriched methane and ethylene as the feedstock to study the reaction between them. The NMR spectra acquired on upon the reaction
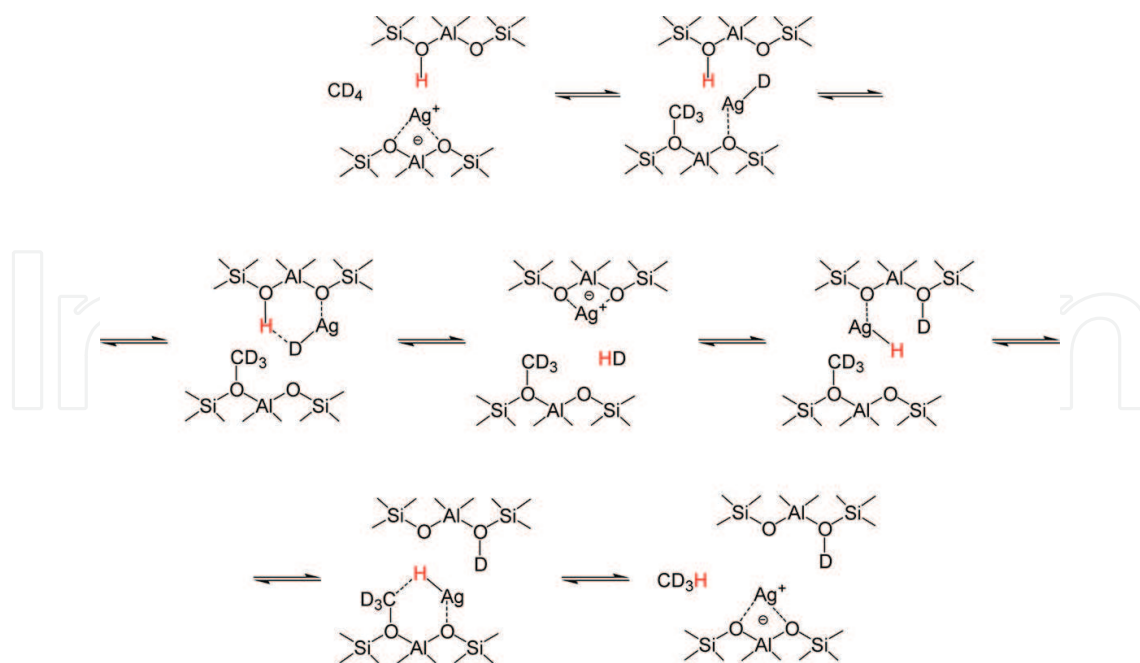
Figure 17. The mechanism of the H/D exchange between methane and brønsted acid sites on Ag/H-ZSM-5 zeolite. Adapted with permission from Ref. [64]. Copyright 2013 American Chemical Society.

between $^{13}CH_4 + CH_2=CH_2$, $^{13}CH_2=CH_2 + CH_4$, and $CH_4 + CH_2=CH_2$ are displayed in **Figure 16**. The peak at 109 ppm is assigned to the ethane π-complex while the signal at 128 ppm is due to the benzene rings of simple alkyl-substituted aromatics adsorbed on zeolite catalysts. By comparing the spectra acquired upon $^{13}CH_2=CH_2$ adsorption and those obtained in the presence of CH_4, it is clear that the introduction creates additional peaks at 623 K (**Figure 16e**), including those belonging to aromatic species. It also significantly enhances the signal intensity due to benzene rings at 823 K (**Figure 16f**). By comparing the spectra acquired using $^{13}CH_4 + CH_2=CH_2$ and $CH_4 + CH_2=CH_2$ (**Figure 16i**, l), it is worth noting that when ^{13}C-enriched methane is present, the signal intensity due to benzene rings is increased dramatically, indicating that a large fraction of benzene product molecules origin from methane. Also, it is noticed that when $^{13}CH_4$ is present with ethene, the peak intensity due to aromatics is much stronger than that obtained when $^{13}CH_4$ is fed without ethene. Such observation indicates that the conversion of methane into aromatics is significantly improved by co-fed ethene.

The authors also propose a possible reaction mechanism (**Figure 17**) to describe the reaction between methane and the catalyst. The hydrogen from methane reacts with H from the brønsted acid sites with the assistance of the Ag active sites.

Similar methods have been practiced on other catalysts that demonstrate outstanding methane activation activity including In/ZSM-5 [65]. By elevating the temperature and acquire the corresponding SSNRM spectra (**Figure 18**), the intermediates from the evolution of methane is identified. Accordingly, the reaction pathway is interpreted **Figure 18e**. Methane dissociates on the In=O site on the catalyst to form H_3C-In=O and brønsted OH groups. The H_3C–In=O then reacts with the In=O site to form H_3C-O-In=O site, which results in benzene, toluene and acetic acid molecules.
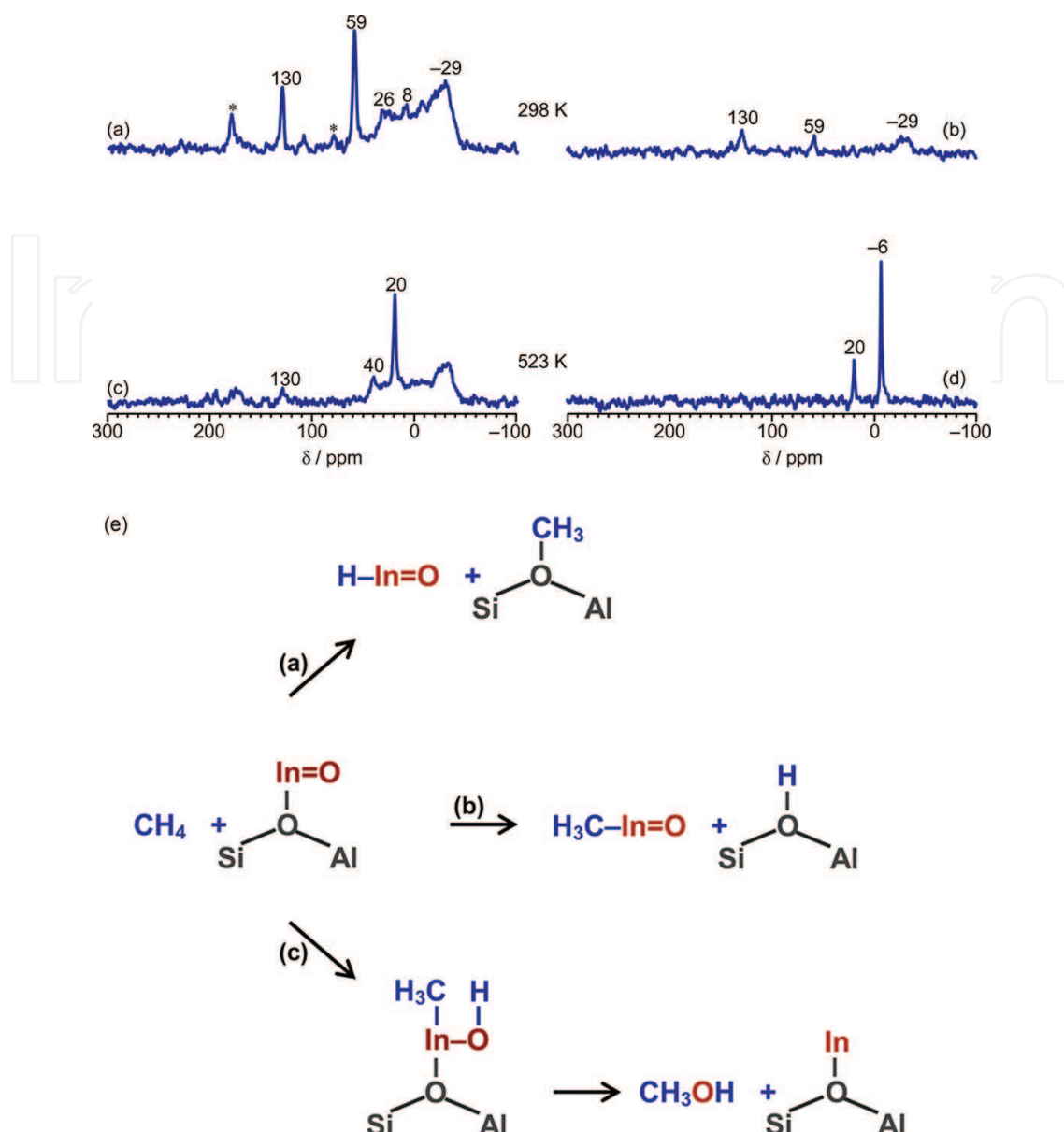
Figure 18. ^{13}C CP/MAS and ^{13}C MAS NMR spectra of surface species generated from methane-^{13}C on InO+/H-ZSM-5 zeolite with co-adsorbed benzene: at ambient temperature (a and b) and after heating at 523 K (c and d). Pathways of methane transformation on InO+/ HZSM-5 zeolite (e). Adapted with permission from Ref. [65]. Copyright 2014 American Chemical Society.

Besides SSNMR, the reaction mechanism is also probed using other methods. For instance, Liu et al. [66] employed a variety of characterization methods including FTIR, temperature-programmed reduction in H_2 (H_2-TPR), temperature-programmed desorption of NH_3 (NH_3-TPD) to study the evolution of methane on Zn/ZSM-5. The proposed reaction pathway is demonstrated in **Figure 19**. The dissociation of CH_4 involves an intermediate of H–CH_3–O–Zn four-member ring (**Figure 19a**). The bond between H and CH_3 would be broken, and the positively charged CH_3 group is bonded to the oxygen belonging to the zeolite framework (**Figure 19b**), followed by the aromatization steps (**Figure 19c**).
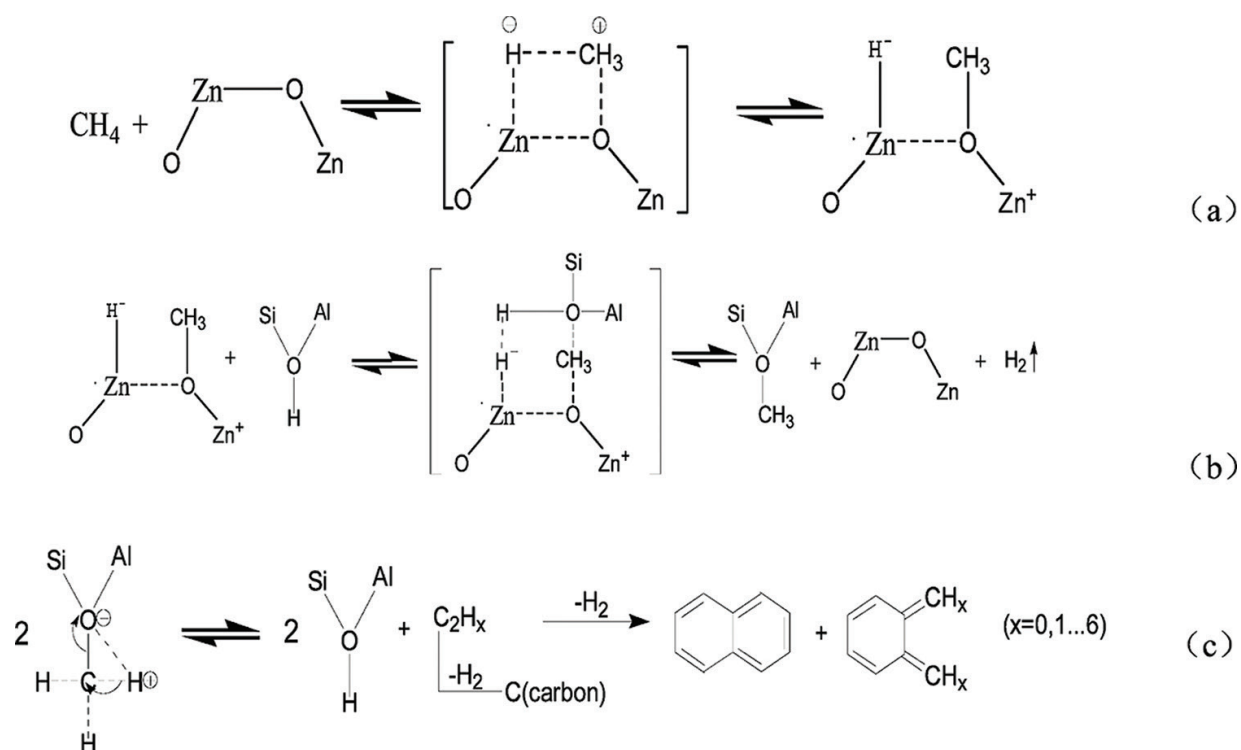
Figure 19. Mechanism of CH$_4$ conversion to aromatic compounds over 2Zn/HZSM-5. Adapted with permission from Ref. [66]. Copyright 2011 American Chemical Society.

In addition to the aromatization of methane, other reactions such as the reaction between methane and CO$_2$ [67] and the one between methane and CO [68] have also been studied using SSNMR. The methane activation pathways in these scenarios help reveal the activation mechanism of methane. Two methane dissociation pathways, i.e., alkyl and carbenium pathways [61], have been revealed. In one scenario, upon the cleavage of C–H bond in CH$_4$, the negatively charged CH$_3$ piece is attached to the active metal, while H is bonded to the oxygen on the catalyst. This pathway is denoted "alkyl pathway". In the other one, CH$_3$ is bonded to an oxygen atom and positively charged. Therefore, it is denoted "carbenium pathway".

5. Computational approaches

The theoretical calculation is a powerful tool to understand and interpret the reaction pathway taking place. The obtained information will guide the rational design of the catalyst to achieve better performance on the oil upgrading using methane. As is demonstrated in previous sections, such feedstock and product matrix are highly complex. Therefore, the theoretical calculation is mainly explored over simpler systems such as the evolution of methane alone. Xu et al. [63] carried out the calculation using the Gaussian 09 software package. Al$_2$Si$_6$O$_9$H$_{14}$ is used as the cluster model to represent the structure of ZSM-5. The negative charges of the cluster are balanced by the positively charged Zn^{2+}, Zn$^+$ and Zn–O–Zn clusters. The energy gaps between each intermediate are displayed in **Figure 20**. It is noticed that the energy of
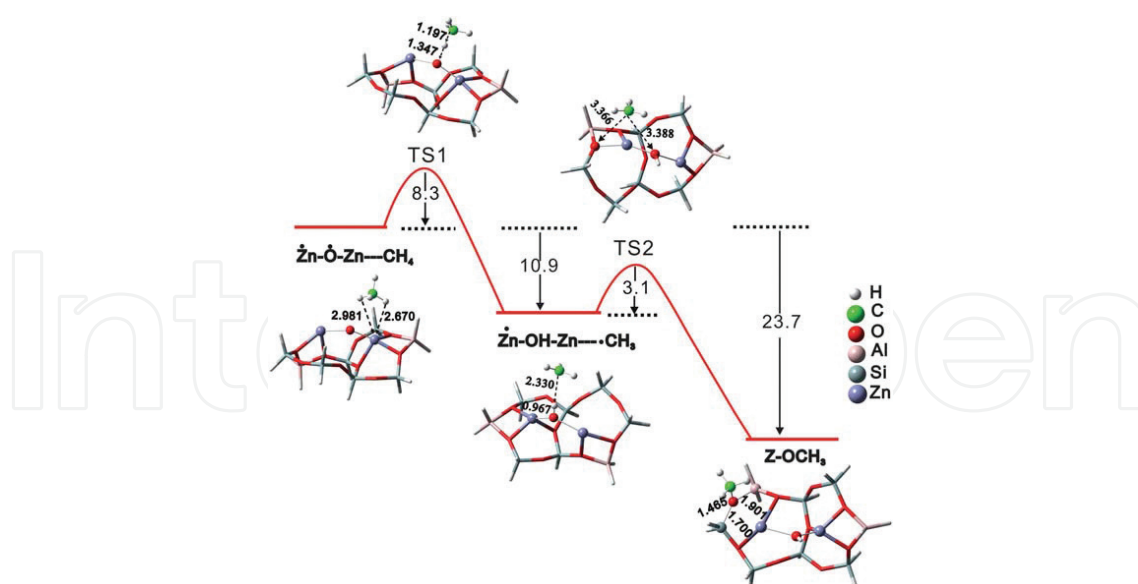
Figure 20. Homolytic cleavage reaction pathway from DFT calculation for the activation of methane on Zn–O–Zn cluster in open shell to produce methoxy intermediates. Calculated energies (kcal mol^{-1}) and selected interatomic distances (Å) are indicated. Adapted from Ref. [63] with permission from the Royal Society of Chemistry.

the structure H$_3$C-O-zeolite is the lowest. Accordingly, this structure is the most stable and possibly the key intermediate during the methane activation and dissociation. This observation also confirms the methane dissociation step in the mechanism proposed by Liu et al. [66] displayed in **Figure 19**.

Mo/ZSM-5 has been intensively studied for methane activation and conversion [69–71]. It has been determined that the active sites on the catalyst are closely related to the molybdenum carbide species [72]. In order to identify the anchoring sites of Mo carbide nanoparticles that catalyze the dehydroaromatization of methane, Gao et al. [73] compared the infrared vibrational spectra for surface OH groups before and after the introduction of Mo species. The anchoring modes of Mo carbide nanoparticles, however, cannot be accurately determined through the IR spectroscopy. DFT cluster calculations and with hybrid quantum mechanical and molecular mechanical (QM/MM) periodic structure calculations are employed to evaluate them. The structures of Mo$_2$C$_x$ (x = 1, 2, 3, 4, and 6) and Mo$_4$C$_x$ (x = 2, 4, 6, and 8) nanoparticles are identified by the calculation results. It is also interesting to note that Mo carbide nanoparticles with a C/Mo ratio >1.5 are more stable on external Si sites according to the calculation results. They tend to migrate from inner pores of the zeolite to the external surface. Therefore, in order to minimize such migration, the researches pointed out that the C/Mo ratio for zeolite supported Mo carbide nanoparticles under hydrocarbon reaction conditions should be maintained below 1.5.

Computational calculation has also been used by many other researchers to gain a better understanding of the reaction thermodynamics [74, 75], reaction intermediates [76–79] and select the most active metal species [80]. This approach should be further developed to obtain more details of the reaction and guide the rational design of the catalyst.

6. Economic considerations

Natural gas, including its recently largely discovered form (shale gas), is abundant in North America. Currently, the utilization of natural gas is often limited to fuels and feedstock used in reforming to produce hydrogen. As a fuel, the application of natural gas is impeded by the difficulties in the liquefaction process. It is challenging to ship the natural oversea to customers in Europe and Asia. As a result, the value of natural gas is significantly underestimated compared with other hydrocarbon resources. According to the Annual Energy Outlook by the US Energy Information Administration in 2015, the price of natural gas is below \$3.73 per million British thermal units (MBTU), while that of gasoline is above \$10.77 per MBTU.

The proposed unconventional oil upgrading using methane, the principal component of natural gas, offers an effective approach to increase the value associated with natural gas by incorporating methane into the synthetic oil molecules. It not only enhances the productivity of the product oil but also converts the low value added methane into high value added commodities, making the process more profitable.

7. Future development

The key to achieve effective upgrading of unconventional oils using natural gas is to deliver at least a catalyst formula that could effectively active methane, crack and rearrange the carbon chains oil molecules and incorporate the cleaved methane pieces into the oil molecules under a relatively low pressure. To be more specific, the catalyst should be able to catalyze the methane dissociation, as well as the addition of the CH_x and H_{4-x} moieties towards the unsaturated bonds of the oil molecules. Olefins in the product oil, which lead to instability issues, could also be diminished by the conversion to aromatics, which requires the aromatization capability of the catalysts to complete this dehydroaromatization process.

It has been evidenced that the activation of methane is assisted by the presence of higher hydrocarbons such as ethane and propylene. Therefore, the catalyst should be able to maximize such synergetic effect. It is also observed that upon the C–H bond cleavage, the CH_3 species may be bonded to the active metal or the oxygen of the framework, depending on the nature of the catalyst. In order to facilitate the activation of methane, the formula of the catalyst should be carefully designed to lower the energy of these intermediates. The optimization of the catalyst might be achieved by tuning the species and concentration of the active metal, surface acidity, as well as the morphology of the support materials including the pore size distribution.

Author details

Peng He and Hua Song*

*Address all correspondence to: sonh@ucalgary.ca

Department of Chemical and Petroleum Engineering, University of Calgary, Calgary, Alberta, Canada

References

[1] Alonso DM, Wettstein SG, Dumesic JA. Bimetallic catalysts for upgrading of biomass to fuels and chemicals. Chem Soc Rev [Internet]. 2012;41(24):8075-98. Available from: http://xlink.rsc.org/?DOI=c2cs35188a

[2] Liu D, Chen EY-X. Organocatalysis in biorefining for biomass conversion and upgrading. Green Chem [Internet]. 2014;16:964-81. Available from: http://pubs.rsc.org/en/content/articlehtml/2013/gc/c3gc41934g

[3] Tuck CO, Perez E, Horvath IT, Sheldon RA., Poliakoff M. Valorization of biomass: deriving more value from waste. Science. 2012;337(6095):695-9.

[4] Van Putten RJ, Van Der Waal JC, De Jong E, Rasrendra CB, Heeres HJ, De Vries JG. Hydroxymethylfurfural, a versatile platform chemical made from renewable resources. Chem Rev. 2013;113(3):1499-597.

[5] Zakrzewska ME, Bogel-Łukasik E, Bogel-Łukasik R. Ionic liquid-mediated formation of 5-hydroxymethylfurfural-A promising biomass-derived building block. Chem Rev. 2011;111(2):397-417.

[6] Gallezot P. Conversion of biomass to selected chemical products. Chem Soc Rev [Internet]. 2012;41(4):1538-58. Available from: http://pubs.rsc.org/en/Content/ArticleHTML/2012/CS/C1CS15147A

[7] Zhang L, Liu R, Yin R, Mei Y. Upgrading of bio-oil from biomass fast pyrolysis in China: A review. Renew Sustain Energy Rev [Internet]. Elsevier; 2013;24:66-72. doi:10.1016/j.rser.2013.03.027

[8] Bridgwater AV. Review of fast pyrolysis of biomass and product upgrading. Biomass Bioenergy [Internet]. Elsevier Ltd; 2012;38:68-94. doi:10.1016/j.biombioe.2011.01.048

[9] Dickerson T, Soria J. Catalytic fast pyrolysis: A review. Energies. 2013;6(1):514-38.

[10] Bridgwater AV. Production of high grade fuels and chemicals from catalytic pyrolysis of biomass. Catal Today. 1996;29(1-4):285-95.

[11] Gutierrez A, Kaila RK, Honkela ML, Slioor R, Krause AOI. Hydrodeoxygenation of guaiacol on noble metal catalysts. Catal Today. 2009;147(3-4):239-46.

[12] Thangalazhy-Gopakumar S, Adhikari S, Gupta RB, Tu M, Taylor S. Production of hydrocarbon fuels from biomass using catalytic pyrolysis under helium and hydrogen environments. Bioresour Technol [Internet]. Elsevier Ltd; 2011;102(12):6742-9. doi:10.1016/j.biortech.2011.03.104

[13] Horne PA, Nugranad N, Williams PT. Catalytic coprocessing of biomass-derived pyrolysis vapours and methanol. J Anal Appl Pyrolysis. 1995;34(1):87-108.

[14] Carlson TR, Cheng Y-T, Jae J, Huber GW. Production of green aromatics and olefins by catalytic fast pyrolysis of wood sawdust. Energy Environ Sci [Internet]. 2011;4(1):145-61. Available from: http://pubs.rsc.org/en/content/articlepdf/2011/ee/c0ee00341g\nhttp://xlink.rsc.org/?DOI=C0EE00341G

[15] Wright MM, Daugaard DE, Satrio JA, Brown RC. Techno-economic analysis of biomass fast pyrolysis to transportation fuels. Fuel [Internet]. Elsevier Ltd; 2010;89(Suppl. 1): S2-10. doi:10.1016/j.fuel.2010.07.029

[16] Graca I, Lopes JM, Cerqueira HS, Ribeiro MF. Bio-oils upgrading for second generation biofuels. Ind Eng Chem Res. 2013;52(1):275-87.

[17] Zhang H, Zheng J, Xiao R. Catalytic pyrolysis of willow wood with Me/ZSM-5 (Me = Mg, K, Fe, Ga, Ni) to produce aromatics and olefins. BioResources. 2013;8(4):5612-21.

[18] Zhang H, Cheng Y-T, Vispute TP, Xiao R, Huber GW. Catalytic conversion of biomass-derived feedstocks into olefins and aromatics with ZSM-5: the hydrogen to carbon effective ratio. Energy Environ Sci. 2011;4:2297.

[19] Zhang H, Zheng J, Xiao R, Shen D, Jin B, Xiao G, et al. Co-catalytic pyrolysis of biomass and waste triglyceride seed oil in a novel fluidized bed reactor to produce olefins and aromatics integrated with self-heating and catalyst regeneration processes. RSC Adv [Internet]. 2013;3(17):5769. Available from: http://xlink.rsc.org/?DOI=c3ra40694f

[20] Zhang H, Nie J, Xiao R, Jin B, Dong C, Xiao G. Catalytic co-pyrolysis of biomass and different plastics (polyethylene, polypropylene, and polystyrene) to improve hydrocarbon yield in a fluidized-bed reactor. Energy Fuels. 2014;28(3):1940-7.

[21] Li X, Li J, Zhou G, Feng Y, Wang Y, Yu G, et al. Enhancing the production of renewable petrochemicals by co-feeding of biomass with plastics in catalytic fast pyrolysis with ZSM-5 zeolites. Appl Catal A Gen [Internet]. Elsevier B.V.; 2014;481:173-82. doi:10.1016/j.apcata.2014.05.015

[22] Zhang H, Carlson TR, Xiao R, Huber GW. Catalytic fast pyrolysis of wood and alcohol mixtures in a fluidized bed reactor. Green Chem [Internet]. 2012;14(1):98-110. Available from: http://xlink.rsc.org/?DOI=C1GC15619E\nhttp://www.scopus.com/inward/record.url?eid=2-s2.0-84855852575&partnerID=tZOtx3y1

[23] Speight JG. Heavy Oil Production Processes. Elsevier; 2013.

[24] Speight JG. Petroleum Refining Processes. Marcel Dekker, Inc.; 2002.

[25] Belyk G, Burgart D, Jablonski B, Heida J, Kaiser T, Bernar R, et al. Heavy Oil 101. Participant Handbook. Canadian Heavy Oil Associations; 2013.

[26] Mech M. A Comprehensive Guide to the Alberta OilSands. 2011.

[27] Bolland JL. Kinetics of olefin oxidation. Q Rev Chem Soc [Internet]. 1949;3(1):1-21. Available from: http://xlink.rsc.org/?DOI=qr9490300001

[28] Xiao Y, He P, Cheng W, Liu J, Shan W, Song H. Converting solid wastes into liquid fuel using a novel methanolysis process. Waste Manag [Internet]. Elsevier Ltd; 2015;49:304-10. doi:10.1016/j.wasman.2015.12.017

[29] He P, Song H. Catalytic Conversion of Biomass by Natural Gas for Oil Quality Upgrading. 2014;

[30] Tan S, Zhang Z, Sun J, Wang Q. Recent progress of catalytic pyrolysis of biomass by HZSM-5. Chin J Catal [Internet]. Dalian Institute of Chemical Physics, the Chinese Academy of Sciences; 2013;34(4):641-50. Available from: http://www.sciencedirect.com/science/article/pii/S1872206712605312

[31] Nie L, Resasco DE. Improving carbon retention in biomass conversion by alkylation of phenolics with small oxygenates. Appl Catal A Gen [Internet]. Elsevier B.V.; 2012; 447-448:14-21. doi:10.1016/j.apcata.2012.08.041

[32] Pham TN, Shi D, Resasco DE. Evaluating strategies for catalytic upgrading of pyrolysis oil in liquid phase. Appl Catal B Environ [Internet]. Elsevier B.V.; 2014;145:10-23. doi:10.1016/j.apcatb.2013.01.002

[33] Elliott DC. Historical developments in hydroprocessing bio-oils. Energy Fuels. 2007;21(3):1792-815.

[34] Laurent E, Delmon B. Influence of water in the deactivation of a sulfided Nimo Gamma-Al_2O_3 catalyst during hydrodeoxygenation. J Catal. 1994;146(1):281-91.

[35] Al-Sabawi M, Chen J, Ng S. Fluid catalytic cracking of biomass-derived oils and their blends with petroleum feedstocks: A review. Energy Fuels. 2012;26(9):5355-72.

[36] Martinez R, Huff MC, Barteau MA. Ketonization of acetic acid on titania-functionalized silica monoliths. J Catal. 2004;222(2):404-9.

[37] Barrett CJ, Chheda JN, Huber GW, Dumesic JA. Single-reactor process for sequential aldol-condensation and hydrogenation of biomass-derived compounds in water. Appl Catal B Environ. 2006;66(1-2):111-8.

[38] Zhao C, He J, Lemonidou AA, Li X, Lercher JA. Aqueous-phase hydrodeoxygenation of bio-derived phenols to cycloalkanes. J Catal [Internet]. Elsevier Inc.; 2011;280(1):8-16. doi:10.1016/j.jcat.2011.02.001

[39] Wildschut J, Mahfud FH, Venderbosch RH, Heeres HJ. Hydrotreatment of fast pyrolysis oil using heterogeneous noble-metal catalysts. Ind Eng Chem Res [Internet]. 2009;48(23):10324-34. doi:10.1021/ie9006003

[40] Baldauf W, Balfanz U, Rupp M. Upgrading of flash pyrolysis oil and utilization in refineries. Biomass Bioenergy. 1994;7(1-6):237-44.

[41] Damartzis T, Zabaniotou A. Thermochemical conversion of biomass to second generation biofuels through integrated process design—A review. Renew Sustain Energy Rev [Internet]. Elsevier Ltd; 2011;15(1):366-78. doi:10.1016/j.rser.2010.08.003

[42] Ma Z, Troussard E, Van Bokhoven JA. Controlling the selectivity to chemicals from lignin via catalytic fast pyrolysis. Appl Catal A Gen [Internet]. Elsevier B.V.; 2012; 423-424:130-6. doi:10.1016/j.apcata.2012.02.027

[43] Pattiya A, Titiloye JO, Bridgwater AV. Evaluation of catalytic pyrolysis of cassava rhizome by principal component analysis. Fuel [Internet]. Elsevier Ltd; 2010;89(1):244-53. doi:10.1016/j.fuel.2009.07.003

[44] Al-Khattaf S, Ali SA., Aitani AM, Žilková N, Kubička D, Čejka J. Recent advances in reactions of Alkylbenzenes over novel zeolites: the effects of zeolite structure and morphology. Catal Rev Sci Eng [Internet]. 2014;56(Sep):333-402. Available from: http://www.tandfonline.com/doi/abs/10.1080/01614940.2014.946846

[45] He P, Shan W, Xiao Y, Song H. Performance of Zn/ZSM-5 for in situ catalytic upgrading of pyrolysis bio-oil by methane. Top Catal [Internet]. Springer, US; 2016;59(1):86-93. doi:10.1007/s11244-015-0508-4

[46] Topsoe H, Clausen BS, Massoth FE. Hydrotreating catalysis. In: Catalysis—Sciences and Technology [Internet]. Berlin, Heidelberg: Springer Berlin Heidelberg; 1996 [cited 2016 Mar 24]. p. 344. Available from: http://linkinghub.elsevier.com/retrieve/pii/S0166983400801335

[47] Kimura N, Iwanami Y, Konno S, Corporation E. Regenerated Hydrotreatment Catalyst. US8795514B2, 2014.

[48] Zakharov I, Startsev A. An ab initio molecular orbital study of the hydrogen sorbed site in Co/MoS$_2$ catalysts. J Phys Chem B [Internet]. 2000;(V):9025-8. Available from: http://pubs.acs.org/doi/abs/10.1021/jp001354f

[49] Breysse M, Portefaix JL, Vrinat M. Support effects on hydrotreating catalysts. Catal Today [Internet]. 1991;10(4):489-505. Available from: https://abingdonsharedfiles.box.com/s/p5c2yhfpvqi3r754qqr7h1p2gnw9plds

[50] Jossens LW, Munson CL. Mild Hydrotreating/Extraction Process for Low Sulfur Gasoline. US6228254B1, 2001.

[51] Lauritsen J. Atomic-scale structure of Co–Mo–S nanoclusters in hydrotreating catalysts. J Catal [Internet]. 2001;197(1):1-5. Available from: http://www.sciencedirect.com/science/article/pii/S0021951700930884

[52] Guo A, Wu C, He P, Luan Y, Zhao L, Shan W, et al. Low-temperature and low-pressure non-oxidative activation of methane for upgrading heavy oil. Catal Sci Technol [Internet]. Royal Society of Chemistry; 2016; doi:10.1039/C5CY00947B

[53] Tsaprailis H, Zhou J. Properties of Dilbit and Coventional Crude Oils [Internet]. Alberta Innovates; 2014. 93 p. Available from: http://www.ai-ees.ca/media/10927/properties_of_dilbit_and_conventional_crude_oils_-_aitf_-_final_report_revised.pdf

[54] Choudhary VR. Low-temperature nonoxidative activation of methane over H-galloaluminosilicate (MFI) zeolite. Science [Internet]. 1997;275(5304):1286-8. Available from: http://www.sciencemag.org/cgi/doi/10.1126/science.275.5304.1286

[55] Guo X, Fang G, Li G, Ma H, Fan H, Yu L, et al. Direct, nonoxidative conversion of methane to ethylene, aromatics, and hydrogen. Science [Internet]. 2014;344(6184):616-9. Available from: http://www.sciencemag.org/content/344/6184/616

[56] Choudhary TV., Aksoylu E, Wayne Goodman D. Nonoxidative activation of methane. Catal Rev [Internet]. 2003;45(1):151-203. Available from: http://www.tandfonline.com/doi/abs/10.1081/CR-120017010

[57] Baba T, Abe Y. Metal cation-acidic proton bifunctional catalyst for methane activation: Conversion of 13CH4 in the presence of ethylene over metal cations-loaded H-ZSM-5. Appl Catal A Gen. 2003;250(2):265-70.

[58] Weckhuysen BM, Wang D, Rosynek MP, Lunsford JH. Conversion of Methane to Benzene over Transition Metal Ion ZSM-5 Zeolites. J Catal [Internet]. 1998;175(2):347-51. Available from: http://www.sciencedirect.com/science/article/pii/S0021951798920115

[59] Borry RW, Kim YH, Huffsmith A, Reimer JA., Iglesia E. Structure and density of Mo and acid sites in Mo-exchanged H-ZSM5 catalysts for nonoxidative methane conversion. J Phys Chem B [Internet]. 1999;103(28):5787-96. Available from: http://pubs.acs.org/doi/abs/10.1021/jp990866v

[60] Luzgin M V., Rogov VA, Arzumanov SS, Toktarev AV., Stepanov AG, Parmon VN. Understanding methane aromatization on a Zn-modified high-silica zeolite. Angew Chem Int Ed. 2008;47(24):4559-62.

[61] Luzgin MV., Gabrienko AA, Rogov VA, Toktarev AV., Parmon VN, Stepanov AG. The "alkyl" and "carbenium" pathways of methane activation on Ga-modified zeolite BEA: ^{13}C solid-state NMR and GC-MS study of methane aromatization in the presence of higher alkane. J Phys Chem C. 2010;114(49):21555-61.

[62] Luzgin MV., Rogov VA, Arzumanov SS, Toktarev A V., Stepanov AG, Parmon VN. Methane aromatization on Zn-modified zeolite in the presence of a co-reactant higher alkane: How does it occur? Catal Today. 2009;144(3-4):265-72.

[63] Xu J, Zheng A, Wang X, Qi G, Su J, Du J, et al. Room temperature activation of methane over Zn modified H-ZSM-5 zeolites: insight from solid-state NMR and theoretical calculations. Chem Sci. 2012;3(207890):2932-40.

[64] Gabrienko AA, Arzumanov SS, Moroz IB, Toktarev A V., Wang W, Stepanov AG. Methane activation and transformation on Ag/H-ZSM-5 zeolite studied with solid-state NMR. J Phys Chem C. 2013;117(15):7690-702.

[65] Gabrienko AA, Arzumanov SS, Moroz IB, Prosvirin IP, Toktarev AV., Wang W, et al. Methane activation on in-modified ZSM-5: the state of indium in the zeolite and pathways of methane transformation to surface species. J Phys Chem C. 2014;118(15):8034-43.

[66] Liu BS, Zhang Y, Liu JF, Tian M, Zhang FM, Au CT, et al. Characteristic and mechanism of methane dehydroaromatization over Zn-based/HZSM-5 catalysts under conditions of atmospheric pressure and supersonic jet expansion. J Phys Chem C. 2011;115(34):16954-62.

[67] Qi G, Xu J, Su J, Chen J, Wang X, Deng F. Low-temperature reactivity of Zn+ ions confined in ZSM-5 zeolite toward carbon monoxide oxidation: insight from in situ DRIFT and ESR spectroscopy. J Am Chem Soc. 2013;135(18):6762-5.

[68] Wang X, Xu J, Qi G, Li B, Wang C, Deng F. Alkylation of benzene with methane over ZnZSM-5 zeolites studied with solid-state NMR spectroscopy. J Phys Chem C [Internet]. Royal Society of Chemistry; 2013;117(8):4018-23. doi:10.1039/C4CC03621B

[69] Abdelsayed V, Shekhawat D, Smith MW. Effect of Fe and Zn promoters on Mo/HZSM-5 catalyst for methane dehydroaromatization. Fuel [Internet]. Elsevier Ltd; 2015;139: 401-10. doi:10.1016/j.fuel.2014.08.064

[70] Ismagilov ZR, Matus EV., Tsikoza LT. Direct conversion of methane on Mo/ZSM-5 catalysts to produce benzene and hydrogen: achievements and perspectives. Energy Environ Sci [Internet]. 2008;1(5):526. Available from: http://pubs.rsc.org/en/content/ articlehtml/2008/ee/b810981h

[71] Wang D, Lunsford JH, Rosynek MP. Characterization of a Mo/ZSM-5 catalyst for the conversion of methane to benzene. J Catal [Internet]. 1997;169(1):347-58. Available from: http://www.sciencedirect.com/science/article/pii/S0021951797917127

[72] Cook B, Mousko D, Hoelderich W, Zennaro R. Conversion of methane to aromatics over Mo2C/ZSM-5 catalyst in different reactor types. Appl Catal A Gen. 2009;365(1):34-41.

[73] Gao J, Zheng Y, Fitzgerald GB, de Joannis J, Tang Y, Wachs IE, et al. Structure of Mo 2 C x and Mo 4 C x molybdenum carbide nanoparticles and their anchoring sites on ZSM-5 zeolites. J Phys Chem C [Internet]. 2014;118(9):4670-9. Available from: http://pubs.acs. org/doi/abs/10.1021/jp4106053

[74] Baba T, Sawada H. Conversion of methane into higher hydrocarbons in the presence of ethylene over H-ZSM-5 loaded with silver cations. Phys Chem Chem Phys. 2002;4(15):3919-23.

[75] Rane N, Kersbulck M, van Santen RA, Hensen EJM. Cracking of n-heptane over Brønsted acid sites and Lewis acid Ga sites in ZSM-5 zeolite. Microporous Mesoporous Mater. 2008;110(2-3):279-91.

[76] Miao S, Wang Y, Ma D, Zhu Q, Zhou S, Su L, et al. Effect of Ag+ cations on nonoxidative activation of methane to C2-hydrocarbons. J Phys Chem B. 2004;108(46):17866-71.

[77] Pidko EA, Hensen EJM, Van Santen RA. Dehydrogenation of light alkanes over isolated gallyl ions in Ga/ZSM-5 zeolites. J Phys Chem C. 2007;111(35):13068-75.

[78] Hensen EJM, Pidko EA, Rane N, Van Santen RA. Water-promoted hydrocarbon activation catalyzed by binuclear gallium sites in ZSM-5 zeolite. Angew Chem Int Ed. 2007;46(38):7273-6.

[79] Li L, Li GD, Yan C, Mu XY, Pan XL, Zou XX, et al. Efficient sunlight-driven dehydrogenative coupling of methane to ethane over a Zn+-modified zeolite. Angew Chem Int Ed. 2011;50(36):8299-303.

[80] Fellah MF, Onal I. C-H bond activation of methane on M- and MO-ZSM-5 (M = Ag, Au, Cu, Rh and Ru) clusters: a density functional theory study. Catal Today [Internet]. Elsevier B.V.; 2011;171(1):52-9. doi:10.1016/j.cattod.2011.04.001